Increased interleukin-11 and stress genes in human endothelial and human bronchial epithelial cell lines by silver nanoparticles

Jiyoung Jang

The Graduate School

Yonsei University

Graduate Program for Nanomedical Science

Increased interleukin-11 and stress genes
in human endothelial and
human bronchial epithelial cell lines
by silver nanoparticles

Directed by Professor In-Hong Choi

A Doctoral Dissertation
Submitted to Graduate Program for Nanomedical Science
and the Graduate School of Yonsei University
in partial fulfillment of the requirements for the degree of
Doctor of Philosophy

Jiyoung Jang

December 2016

This certifies that the Doctoral Dissertation of

Jiyoung Jang is approved.

Thesis Supervisor : In-Hong Choi

Thesis Committee Member #1 : Dong-Chun Shin

Thesis Committee Member #2 : Kangtaek Lee

Thesis Committee Member #3 : Ji-Yeon Yang

Thesis Committee Member #4 : Sun Park

The Graduate School Yonsei University

December 2016

ACKNOWLEDGEMENTS

처음 박사과정에 입문한 날로부터 비로소 모든 과정을 마치는 지금까지의 순간들을 되돌아보며 도움 주신 많은 분들께 감사의 글을 남깁니다.

이렇게 결실을 맺기까지 부족한 저를 이끌어주시고 많은 기회를 주신 최인홍 교수님, 교수님을 향한 감사의 마음은 글로써는 다 표현할 수 없을 것 같습니다. 교수님의 지도와 이끌어 주심에 학위과정을 끝까지 마칠 수 있었습니다. 박사과정 동안 교수님의 가르침을 통해 나노독성과 면역학에 한 발짝 더 다가갈 수 있었고, 학문에 대한 다양한 발상과 연구에 매진하시는 모습을 통해 많은 깨달음을 얻었습니다. 그 동안 주신 따뜻한 마음과 가르침 평생 잊지 않고 살아가겠습니다. 진심으로 감사 드립니다. 지금의 제가 시작될 수 있게 발판을 마련해 주신 신동천 교수님, 환경공해연구소에서의 생활을 통해 독성학을 접할 수 있었고 다양한 분야를 경험하면서 넓은 지식을 쌓을 수 있게 도움 주셔서 너무나도 감사 드립니다. 그리고 나노물질에 대한 공학적인 지식과 조언을 아끼지 않으신 이강택 교수님, 바쁘신 와중에도 부족한 제 논문을 꼼꼼히 검토해 주시고 방향을 잡아주신 양지연 교수님, 박선 교수님께도 깊은 감사를 드립니다.

미생물학교실에서 함께 생활하며 다방면으로 도움을 주신 여러 선생님들 역시 깊은 감사를 드립니다. 함께한 시간들이 가장 많은 스마트한 진원씨, 조용하고 듬직한 한구, 밝고 부지런한 수민이, 양은정 박사님, 장영생 박사님 모두 감사 드립니다. 저에 대해 너무나도 많은 것을 알고 있는 30 년지기 단짝 친구

안선영, 똑 부러지는 어린 친구 송경주, 이상하게 정이 가는 김수환 양에게도 고마움의 인사를 전합니다.

 무엇보다도 저의 존재의 이유인 사랑하는 우리 가족들에게도 감사 드립니다. 학위과정 중에 결혼과 출산을 하면서 많이 흔들렸던 저를 다잡아주신 친정 부모님, 두 분의 도움 없이는 절대 불가능했을 박사학위 입니다. 특히나 친정엄마께 너무나도 깊은 감사를 드립니다. 이젠 결혼해서 가정을 꾸린 남동생 동균이, 늘 열심히 하는 모습이 보기 좋다고 하시는 시댁 부모님, 형님께도 감사 드립니다. 그리고 제 옆의 가장 든든한 언제까지나 내편인 우리 신랑과 웃는 얼굴이 너무 예쁜 우리 딸 예진이에게도 고맙고 사랑한다는 말 전합니다.

 이 외에 제가 미처 언급하지 못한 고마운 분들이 너무나 많습니다. 그분들의 이름을 모두 새기지 못함을 죄송스럽게 생각하며, 대신 제 깊은 감사의 말로 이 글을 마칩니다. 진심으로 감사 드립니다.

<div align="right">

2016 년 12 월

장지영 사룀

</div>

CONTENTS

LIST OF FIGURES

Ⅰ. Human endothelial cell

Ⅱ. Human bronchial epithelial cell

LIST OF TABLES

Ⅱ. Human bronchial epithelial cell

ABBREVIATION

CO   Carbon monoxide

DEG   Differentially expressed gene

DLS   Dynamic light scattering

DMEM   Dulbecco's modified Eagle's medium

DNA   Deoxyribo nucleic acid

ELISA   Enzyme-linked immunosorbent assay

FBS   Fetal bovine serum

GAPDH   Glyceraldehyde 3-phosphate dehydrogenase

GSH   Glutathione

HO-1   Heme oxygenase 1

HSP   Heat shock protein

IL   Interleukin

LD_{50} Lethal Dose 50

MDA   Malondialdehyde

MEM   Minimum Essential Medium

MT   Metallothionein

NPs   Nanoparticles

O.D   Optical density

PVP   Polyvinylpyrrolidone

RefSeq   Reference Sequence

RMA   Robust Multi-array Average

ROS   Reactive oxygen species

RT-PCR   Real-time reverse transcriptase polymerase chain reaction

SD   Standard deviation

ABSTRACT

Increased interleukin-11 and stress genes

in human endothelial and

human bronchial epithelial cell lines

by silver nanoparticles

Jiyoung Jang

Graduate Program for Nanomedical Science

The Graduate School Yonsei University

(Directed by Professor In-Hong Choi)

The ultrafine particle size of nanomaterials is limited to approximately 100 nm, and such a small size has allowed nanomaterials to be used in a variety of ways. Therefore, engineered nanoparticles are being used in various industries, including ceramics, polymers, smart textiles, pharmaceutical products, cosmetics, biomedicine, electronics, paints,

chemicals, food, and environmental analysis. Metal nanoparticles that contain gold, silver, iron, zinc, and metal oxides are widely used for their large surface area to volume ratios and their unique physicochemical properties. In particular, silver NPs are in especially wide use in the medical field, where they are used in diagnosis and treatment and incorporated into medical devices and pharmaceuticals. Interestingly, however, silver NPs have been identified as a cause toxicity in the human body. Because of their small size, NPs that enter the human body can easily penetrate biological barriers and can be circulated throughout the entire body, ultimately reaching the vascular endothelium.

With this in mind, the present study aimed to identify various cell responses by distinguishing between endothelial and epithelial cells and exposing them to silver nanoparticles (NPs). The study also worked to identify the progression of cell apoptosis that occurs as a result of intracellular oxidative stress caused by silver NPs and to determine which genes are being stimulated in order to cause such changes. We also assessed several gene expression levels that increased significantly in the microarray assay.

We evaluated the cytotoxic effects of silver NPs both endothelial and epithelial cells. Although the LD_{50} of each cell line was estimated differently, we were able to prove the toxicity of silver NPs. Meanwhile, for 100 nm silver NPs, cell death was not observed in the high concentration group. We verified through microarray that 5 nm silver NPs affect the

variation of gene expression in cells, and a noticeable increase in the expression of interleukin (IL)-8 and IL-11 genes in early time was also verified. This study found that the variation in oxidative stress-related genes in early time, and among them the variation of metallothionein (MT), heme oxygenase 1 (HO-1), and heat shock 70kDa protein (HSP70) expression, was noticeable. This study proves that HSP70, HO-1, and MT are sufficient as biomarkers of reactive oxygen species (ROS) and that the oxidative stress effect is greater as the size of NPs is smaller assuming that there is no variation in ROS related gene expression in 100 nm silver NPs. The microarray used in this study can analyze up to 24,838 RefSeq (Entrez) genes. Based on this analysis, genes undergoing intracellular change after exposure to silver NPs were classified into five categories: cell death, cell survival, inflammation, apoptosis, and ROS. As a result, there was considerable variation in genes related to cell death and apoptosis, and the expression of genes related to cell survival was also not negligible. Meanwhile, the number of genes related to inflammation was relatively small. Moreover, what is especially worth paying attention to is the increased IL-11 gene expression, which has not been much discussed in previous studies. In this study, the IL-11 gene expression particularly increased following the exposure of endothelial and epithelial cells to 5 nm silver nanoparticles. This study therefore verifies that IL-11 expression commonly increases in cells under the influence of silver NPs.

In conclusion, this study finds that intracellular genes specifically

respond to exposure to silver NPs and that the expression of IL−11 among cytokines is noticeable. It also finds that the toxic effect is affected by the size of NPs. However, this study verifies only that IL−11 expression increased, and thus further study would be required to elaborate on the various roles played by IL−11.

1. Introduction

The ultrafine particle size of nanomaterials is limited to approximately 100 nm, and such a small size has allowed nanomaterials to be used in a variety of ways. In contrast, fine particles have sizes that range from 100 and 2,500 nm (1). Advancements in nanotechnology have led to tiny-scale substances having a significant impact on our lives. Today, nanotechnology is one of the leading scientific fields, combining the fields of physics, chemistry, biology, medicine, pharmaceutical science, informatics, and engineering to establish another major scientific field (2). Nanotechnology represents a dynamic emerging field, with 50,000 or so articles being published each year, and according to the European Patent Office more than 2,500 patents have been filed in recent times (3).

Owing to their excellent usability, engineered nanoparticles are being used in various industries, including ceramics, polymers, smart textiles, pharmaceutical products, cosmetics, biomedicine, electronics, paints, chemicals, food, and environmental analysis (4). In particular, metal nanoparticles that contain gold, silver, iron, zinc, and metal oxides are widely used for their large surface area to volume ratio and their unique physicochemical properties, including a high electrical and thermal conductivity and optical, magnetic, and catalytic activity (5, 6). According to a recent report, about 29% of consumer products in the consumer

1

products inventory (including water, lotion, oil, and car lubricants) contain nanomaterials suspended in a variety of fluids. The second largest group in this category comprises solid products with surface-bound nanoparticles such as curling irons, flat irons, and textiles (7). Among them, the antimicrobial and antifungal effects of silver nanoparticles (NPs) have led to the rapid develop of consumer products applications, and the number of worldwide products based on silver NPs has reached over 313 (5). Silver NPs are in especially wide use in the medical field, where they are used in diagnosis and treatment and incorporated into medical devices and pharmaceuticals. Moreover, silver NPs are widely used for to coat medical tools as well as to sterilize of materials in hospitals (2). In addition, in many products different nanomaterials are combined with others. Silver and titanium dioxide are the nanomaterial components most likely to be combined with other nanomaterials in consumer products, with 35 and 30 product combinations, respectively. Silver and titanium dioxide were paired with each other in 10 products (mostly cosmetics and electronics); titanium dioxide and zinc oxide were paired in 10 products (mostly sunscreens, cosmetics, and paints). The European Commission's Cosmetics Regulation has permitted the use of nanoscale titanium dioxide in sunscreens, but not zinc oxide (7).

However, an interesting point is that silver NPs have been identified as a cause of toxicity in the human body; they are therefore dual-natured, with both positive and negative aspects. Consequently, many researchers are

2

conducting toxicity evaluations and risk assessments of NPs.

All NPs are taken up by mammalian cells by such mechanisms as pinocytosis, endocytosis dependent on caveolae and lipid raft composition, clathrin-dependent endocytosis, and phagocytosis (8), and silver NPs are no exception in this respect. As some studies have shown, normal human lung fibroblasts (IMR-90) and human glioblastoma (U251) take up silver NPs by clathrin-dependent endocytosis and macropinocytosis. In the case of silver NPs (6-20 nm), they were usually present inside cells after a 2 h treatment; uptake was linear during 2 h - 48 h exposure and was the result of a balance between exo- and endocytosis (8).

In one study, toxicoproteomic evaluation following exposure to silver NPs showed an altered pattern of protein expression (9), indicating that silver NP toxicity can cause pathological changes in the human body. A recent study reported that the surface charge of silver NPs was associated with silver NP toxicity (10). The degree of human toxicity can vary depending on the size of the NPs to which the body is exposed. When macrophages were exposed to 5 nm and 100 nm silver NPs, the group exposed to 5 nm silver NPs showed an increase in interleukin-8 expression even early in the exposure and at low concentrations where cell death did not occur. This indicated that smaller NPs can have an inflammatory effect on the intracellular immune system (11). Silver NPs also stimulate cytotoxic mechanisms, producing an indirect effect on the release of lactate from hepatoma cells. One study reported that reactive oxygen species (ROS)

were generated through the secondary influence of NPs, not through their direct influence, which resulted in proportionate decreases in lactate release (12). According to another study, exposing rat liver epithelial cells to silver NPs resulted in a significant increase in intracellular ROS concentration and a decrease in glutathione (GSH) levels, but it was unclear as to whether this was due to GSH directly binding with silver NPs or to GSH synthesis being inhibited by enzymes. A dose-dependent decrease in mitochondrial membrane potential was also found, and cell viability was also noted to be associated with NP exposure, but whether this was attributable to the influence of NPs or Ag^+ ions was not clearly identified (13). Another study examined the cytotoxic effects of silver NPs on human liver cells. The study results showed that silver NPs caused damage to cellular components by inducing ROS generation and reducing GSH levels as well as by causing DNA breakage, lipid peroxidation, and protein carbonylation. Based on these findings, the study concluded that silver NPs are involved in the GSH depletion mechanism and that their presence induces the mitochondria-dependent apoptotic pathway (14). In a recent study, human umbilical vein endothelial cells (HUVECs) were treated with 6 types of NPs. The most noticeable aspect of that study is that the endothelial cells were exposed to NPs by applying a flow system. In most *in vitro* experiments, tests were performed under static conditions, whereas this study exposed the cells to NPs under fluid conditions. This experimental setting was closest to the actual situation of NPs being

exposed to human tissues as they move through the circulatory system in the human body, and the results show that silver NPs were most toxic: silver NPs not only caused inflammation and activation of an IL−8 dependent pathway but also induced pro−apoptotic signals that led to cell apoptosis. Moreover, endothelial cells were more sensitive to silver NPs under flow conditions. The authors of that paper suggest that a physiologically−related *in vitro* model was needed in order to understand the hazards of NPs (15). In addition to these studies, a few other *in vitro* studies have also reported that increasing the exposure of macrophages and human peripheral blood mononuclear cells to silver NPs resulted in the release of various cytokines (16, 17, 18).

Many nanotoxicology studies have focused on the *in vitro* cell culture system. However, the data from these studies could be misleading, and it is difficult to view the results as a whole of organism response. Animal studies (*in vivo* models) are very helpful for understanding the chemical properties of nanomaterials and the response relationship between organisms, including humans. Using an *in vivo* system can provide some basic information on the pathway that NPs use to move through the body after exposure (19). In animal studies, silver NPs are usually applied in a suspended state, allowing Ag^+ ions to be released from the suspension. However, it is still unclear whether the signs of toxicity that result from exposure to silver NPs is due to the small size of the NPs, the silver ions generated in the suspended state, or a combination of both (20). In a 2010

study of toxicity and inflammation response following silver NP exposure in mice, the authors repeated oral administration of silver NPs of different sizes (22, 42, 71, 323 nm) to mice for 14 days. According to the results, silver NPs of different sizes were distributed in various tissues, with small-sized silver NPs appearing even in the brain, lungs, liver, kidney, and testes, whereas such a pattern was not found in the group treated with large-sized 323 nm silver NPs. In addition, when varying concentrations of 42 nm silver NPs were orally administered repeatedly for 28 days, the groups treated with higher concentrations showed an increase in markers indicative of liver damage. Based on these results, the authors concluded that silver NPs are capable of causing hepatotoxicity, though histopathological changes in the liver were not found. On the other hand, oral administration resulted in distinct increases in inflammatory responses, including increased cytokine production and increased B cell distribution (21). However, a subsequent study that contradicted these findings was also published. In that study, observations were made after 28 days of exposure to non-coated silver NPs, polyvinylpyrrolidone (PVP)-coated silver NPs, and Ag ions. Contrary to the previous study, the results showed no liver damage, while blood, lymphocyte proliferation, and cytokine release showed little difference against the control, which indicated no hepatotoxicity or immunotoxicity from silver NP exposure. The authors suggest that the reason for their not finding toxicity despite exposing the mice to highly concentrated silver NPs for a sufficient amount of time was

due to accumulation or agglomeration between particles (22). Most nanoparticles that are actually introduced into the body, whether by inhalation or by other methods of exposure, end up accumulating in the body. However, even if the size increases from accumulation, because they accumulate in varying sizes, it cannot be simply ignored. Researchers have also performed *in vivo* tests of the effect of silver NPs on zebra fish. Exposing zebra fish embryos to 30 to 72 nm silver nanoparticles resulted in nanoparticles spreading slowly within the embryos, which also exhibited size-dependent nanotoxicity (23).

Because of their small size, NPs that enter the human body can easily penetrate biological barriers (skin, intestines, lungs, etc.) and can be circulated throughout the entire body, ultimately reaching the vascular endothelium. Some studies have shown that inhaled nano-sized particles can move through the bloodstream and can spread to the lungs and other organs by passing freely between alveolar epithelial cells and the vascular endothelium through the gap fenestration pathway in the air-blood barrier, which has gaps of 0.03 - 3 μm (24). The endothelium is the human body's first internal layer of blood vessels and is distributed throughout the entire body. Therefore, the first important aspect of the endothelium is that it allows molecules to move to and circulate through various tissues through blood flow. Moreover, the endothelium also controls certain pathways, such as lipid metabolism and vascular inflammation. When these functions are lost, vascular diseases may be triggered (25). These characteristics of the

7

endothelium are closely linked to the mechanism by which NPs infiltrate the human body and make their way to various organs. Accordingly, the present study makes a distinction between epithelial and endothelial cells in observing the toxic effects of silver NPs.

One study shows the effects of silver NPs at the cellular level and summarizes the present state of knowledge. As is the case with other nanoparticles, the most important apparent effect is oxidative stress. The enhanced generation of ROS affects the mitochondrial respiratory chain and increases the amount of unfolded and misfolded proteins in the endoplasmic reticulum, inducing ER stress and the unfolded protein response. Both these types of cellular damage lead to further ROS generation, DNA damage, and the activation of signaling resulting in various cell type−specific pathways to inflammation, apoptosis, or necrotic death (26). Among these ROS pathways, the heat shock response is a major pathway by which the cells protect themselves from oxidative stress, and when cells are damaged, transcriptional upregulation of genes that encode heat shock proteins (HSPs) occurs. HSPs are known as molecular chaperones that play an essential role in folding nascent proteins and deleting misfolded proteins (27). Moreover, HSPs are also involved in regulating mitochondrial membrane integrity, in the activation of caspase, and in various forms of cellular signaling, such as the apoptotic signaling pathway (28). Among HSPs, HSPs that are elevated by stress (HSPA1A, HSP70) are upregulated by pathophysiological stressors like ischemia and have also been reported

to show increased expression from environmental stressors like air pollutants (29, 30, 31). Expression of HSP responds sensitively to stress, and thus is commonly used as a potential biomarker for toxicity.

Heme oxygenase 1 (HO-1) is an inducible enzyme that primarily performs antioxidant and anti-inflammation functions (32). HO-1 is upregulated by various oxidizing agents, heavy metals, pro-inflammatory cytokines, and hypoxia (33, 34, 35). In one study it was shown that bilirubin and carbon monoxide (CO) could be produced by inducing anti-inflammation through the catalytic action of HO-1 (36). Therefore, HO-1 acts as an important factor that protects cells from oxidative stress. Accordingly, the present study aimed to use levels of HSP70 and HO-1 expression in explaining the oxidative stress response generated when exposing cells to the causative substance of silver NPs.

Cytokines are small secreted proteins that control interaction and signaling between cells. Cytokines that play an important role in cell signaling include lymphokines (cytokines produced by lymphocytes), monokines (cytokines produced by monocytes), chemokines (cytokines with chemotactic activities), and interleukins (ILs, cytokines produced by leukocytes to affect the behavior of other leukocytes; however, at present it is clear that all cells are able to secrete cytokines). Although cytokines are secreted from a wide variety of cells, they are secreted in distinctly higher concentrations from helper T cells and macrophages (37). Cytokines possess both pro- and anti-inflammatory properties, but their roles

9

change slightly depending on the situation. Some cytokines, such as interleukin (IL)-1β, IL-6 and TNF$-\alpha$, function as pro-inflammatory cytokines and accompany pathological pain. Chemokines increase chemotaxis, while other cytokine groups show anti-inflammatory effects. IL-1 receptor antagonists (IL-4, IL-10, IL-11, and IL-13) are the primary anti-inflammatory cytokines (37).

IL-11 is a member of the IL-6 family of cytokines and has various functions. The IL-6 family of cytokines includes not only IL-11 but also IL-6, IL-27, IL-31, leukemia inhibitory factor, ciliary neurotrophic factor, oncostatin M, and cardiotrophin-1 (38). IL-6 is associated with chronic inflammatory diseases and is responsible for the progression of various types of cancer. It activates the signal transducer and the activator of transcription 3 (STAT3) pro-survival pathways. According to one study, IL-6 and IL-11 were responsible for advancing gastrointestinal cancer, and during this process IL-11 was found to be closely associated with STAT3 activation (39). IL-11 performs hematopoietic functions in in many different areas of the body, including the liver, the gastrointestinal tract, the lungs, the heart, the central nervous system, the bones, the joints, and the immune system (40). Playing a protective role by accelerating platelet recovery and reducing inflammatory responses, IL-11 was able to lower the mortality rate among sepsis patients (41). In other words, among the immune responses of IL-11, anti-inflammatory properties were also identified. Consequently, the various functions and roles of IL-11 are

drawing new attention. Other biological activities of IL-11 include stimulation of erythropoiesis and activation of megakaryocytes. Moreover, it controls the polarization of T cells and macrophages and promotes the maturation of bone resorbing osteoclasts (42). In addition, it also plays a role in neurogenesis (43), adipogenesis (44), and promotion of stem cell development (45), while also protecting cells from graft versus host disease (46) and blocking gastric acid secretion (47). Finally, IL-11 performs a variety of functions in various cells. In the epithelial cells examined in the present study, IL-11 reduces proliferation and induces apoptosis. Moreover, in endothelial cells it plays a role in cell activation and in the expression of surviving proteins that are involved in cell proliferation. IL-11 also affects mast cells, inducing proliferation. Moreover, in macrophages and osteoclasts, respectively, IL-LL reduces the production of IL-1β, IL-12, NO, NF-κB and decreases formation, increases bone resorption (48).

Based on the above, the present study aimed to identify different types of cell responses by distinguishing between endothelial and epithelial cells and exposing them to silver NPs. The study also aimed to describe the progression of cell apoptosis from the occurrence of intracellular oxidative stress caused by silver NPs and to identify which genes are being stimulated to cause such changes. We also assessed several gene expression levels that increased significantly in the microarray assay. These results provide important insight to help understand and identify the

effects of silver NPs.

2. Materials and Methods

2.1. Effects of silver NPs on endothelial cells (EA.hy926)

2.1.1. Silver NPs

Silver NPs in water-based solutions were obtained from Dr. Koh (5 nm; PNM, Hwaseong, Korea) or purchased from ABC Nanotech (100 nm; Daejeon, Korea). Silver NPs (5 nm and 100 nm) were synthesized by the reduction of $AgNO_3$. All silver NPs were round and PVP-coated. Endotoxin contamination tests were conducted using the Pyrotell®-T kinetic turbidimetric method (Associates of Cape Cod, Inc., MA, USA), and the results were negative (endotoxin < 0.01 U/mL). For cell culture, different concentrations of silver NPs were prepared in high glucose Dulbecco's Modified Eagle's Medium (DMEM; Welgenen, Gyeongsan, Korea) with 2 mM L-glutamine supplemented with 10% fetal bovine serum (FBS; Welgenen), 100 U/mL penicillin, and 100 μg/mL streptomycin.

2.1.2. Characterization of silver NPs

The diameter of the silver NPs was determined using a transmission electron microscope (TEM; model JEM-2010, JEOL Ltd., Tokyo, Japan). Agglomeration of the NPs in DMEM with 10% FBS at 0.5 ㎎/mL was examined by dynamic light scattering (DLS; Malvern Instruments, Novato, CA, USA).

2.1.3. Cell lines and culture

The human umbilical vein cell line, EA.hy926 (ATCC, Manassas, VA, USA), was established by fusing primary human umbilical vein cells with a thioguanine-resistant clone of A549 by exposure to polyethylene glycol (PEG). EA.hy926 cells were cultured in DMEM containing 10% FBS and penicillin-streptomycin (100 U/mL and 100 ㎍/mL, respectively) at 37℃ in a humidified 5% CO_2 atmosphere in an incubator. The culture medium was changed every two to three days to maintain cell density at approximately 1×10^5 cells/cm^2. Although endotoxins were not detected in the silver NPs used in this study, polymyxin B (InvivoGen, San Diego, CA, USA) at a concentration of 10 ng/mL was added as an endotoxin neutralizer.

2.1.4. Analysis of cell proliferation

Cell viability was assessed using the colorimetric cell counting kit-8 (CCK-8; Dojindo Laboratories, Kyoto, Japan). CCK-8 is a colorimetric assay that uses a highly water soluble tetrazolium salt, WST (8[2-(2-methoxy-4-nitrophenyl)-3-(4-nitrophenyl)-5-(2,4-disulfophenyl)-$2H$-tetrazolium, monosodium salt]). Cells were plated in 24-well plates at a density of 5×10^4 cells per 500 μL of growth medium per well and incubated overnight in a 5% CO_2 incubator. The medium was removed and the cells were treated with 500 μL of silver NP solution diluted in the growth medium. After 24 h, 15 μL of the CCK-8 reagent was added to each well and then incubated at 37℃ for 2 h. After 13,000 rpm, 5 min centrifugation, 200 μL of supernatant was transferred to 96-well microtiter plates and the optical density (O.D) was measured at 450 nm with a spectrophotometer (BioTek Instruments, Winooski, VT, USA) to ensure that there was no optical interference by silver NPs.

2.1.5. Cytokine detection

Enzyme-linked immunosorbent assay (ELISA) was used to detect the presence of the cytokines IL-8 and IL-11. EA.hy926 cells were plated in 6-well plates at a density of 1.5×10^5 cells per well in 2 mL of DMEM

containing 10% FBS. The medium was removed and the silver NPs suspended in the medium were added to each well, to a final volume of 1 mL per well. These wells were then incubated for 8 h (for IL-8 assay) and 24 h (for IL-11 assay). After 8 h, the cell culture supernatant was collected and stored at -80℃. ELISA was performed using a human cytokine IL-8 assay kit (BD Biosciences, San Diego, CA, USA). After 24 h, the cell culture supernatant was collected and stored at -80℃. ELISA was performed using a human cytokine IL-11 assay kit (R&D Systems, Minneapolis, MN, USA). These kits use biotinylated anti-IL-8 or anti-IL-11 antibodies and streptavidin conjugated to horseradish-peroxidase. The O.D was measured at 450 nm.

2.1.6. Real-time reverse transcriptase polymerase chain reaction (RT-PCR)

cDNA was synthesized from total RNA via reverse transcription with random primers (Invitrogen, San Diego, CA, USA). Primer pairs designed to amplify the cDNA encoding the target genes were prepared using the Invitrogen Oligo Perfect Designer (Thermo Fisher Scientific, Waltham, Massachusetts, USA). PCR reactions were performed using FastStart Universal SYBR Green Master (ROX) reagent according to the manufacturer's instructions (Roche Applied Science, Mannheim, Germany) in a 7500 and StepOne Plus Real-time PCR system (Applied Biosystems, Foster City, CA, USA). The reaction parameters were as follows: 2 min at

50℃, 10 min at 95℃, 40 cycles of denaturation at 95℃ for 15 s, and 60℃ for 1 min. Real-time RT-PCR data for each gene product were normalized against levels of glyceraldehyde 3-phosphate dehydrogenase (GAPDH). All transcript levels were reported as mean ± standard deviation (SD) relative to untreated controls from triplicate analyses. Gene expression levels were analyzed using the comparative C_T Method with the fold difference calculated based on the endogenous control (GAPDH). Primer sequences were as follows: IL-8, forward: 5'-GTG CAG TTT TGC CAA GGA GT-3' and reverse: 5'-CTC TGC ACC CAG TTT TCC TT-3'; IL-11, forward: 5'-CTG AGC CTG TGG CCA GAT A-3' and reverse: 5'-AGC TGT AGA GCT CCC AGT GC-3'; HO-1, forward: 5'-ATG ACA CCA AGG ACC AGA GC-3' and reverse: 5'-GTG TAA GGA CCC ATC GGA GA-3'; HSP-70, forward: 5'- AGG CCA ACA AGA TCA CCA-3' and reverse: 5'-TCG TCC TCC GCT TTG TAC TT-3'; GAPDH, forward: 5'-GAT CAT CAATGC CTC CT-3' and reverse: 5'-TGT GGT CAT GAG TCC TTC CA-3'. One-way analysis of variance (ANOVA) was used to assess differences between the control and experimental groups.

Formulae: $\Delta C_T = C_{T\ target} - C_{T\ GAPDH}$

$\Delta \Delta C_T = \Delta C_T$ test sample $- \Delta C_T$ control sample

S (standard deviation) $= \sqrt{(S^2_{target} + S^2_{GAPDH})}$

$$\text{Fold difference} = \frac{2^{-(\Delta\Delta C_T + s)} + 2^{-(\Delta\Delta C_T - s)}}{2}$$

2.1.7. Western blot

For western blot analysis, 4.5×10^5 EA.hy926 cells were seeded into 60-mm Petri dishes. Cells were then treated with 5 nm and 100 nm silver NPs for 24 h. Cells were harvested and lysed at 4℃ for 2 h in 200 µL of lysis buffer (150 mM NaCl, 1% NP-40, 0.1% SDS, 50 mM Tris pH 8, 5 mM NaF, 1 mM Na₃VO₄, 1 mM PMSF, protease inhibitor cocktail). The cell lysates were centrifuged at 13,000 rpm for 15 min at 4℃ and the supernatants were stored at −20℃. Protein concentrations in the lysates were measured using the Bradford assay. From each sample, 30-40 µg of protein was boiled for 5 min and loaded on a 12% sodium dodecyl sulfate (SDS)-polyacrylamide gel. After electrophoresis, proteins in the gel were transferred onto nitrocellulose membranes (Amersham, Glattbrugg, Switzerland). After blocking with 5% skim milk (BD Biosciences, Franklin, NJ, USA), membranes were reacted with primary antibodies such as anti-HO-1 antibodies (Cell Signaling Technology, Danvers, MA, USA) and anti-HSP-70 antibodies (Cell Signaling Technology) at 1:1000 dilution in 5% bovine serum albumin (BSA) (Affymetrix, Cleveland, Ohio, USA) at 4℃ overnight. After washing, the membranes were further reacted with a secondary antibody (peroxidase-conjugated affinipure goat anti-rabbit IgG, Jackson ImmunoResearch, West Grove, PA, USA) at 1:2000 dilution in 5%

skim milk at room temperature for 1 h. Protein bands were detected using a Westsave up western blot detection kit (Ab Frontier, Seoul, Korea). An anti-GAPDH antibody (Cell Signaling Technology) was used to assess transcription levels of housekeeping genes. The membranes were exposed to X-ray film (Fujifilm, Tokyo, Japan). Each band was analyzed using the software ImageJ (https://imagej.nih.gov/ij/). Fold induction was calculated as follows: fold induction = densitometric value of study group / densitometric value of control group.

2.1.8. Transmission electron microscopy (TEM) analysis

EA.hy926 cells treated with 1.5 μg/mL of 5 nm and 100 nm silver NPs for 30 min were fixed with Karnovsky solution (2.5% glutaraldehyde, 2% paraformaldehyde, 0.5% $CaCl_2$) for 1 h and then washed three times with PBS buffer. Cells were treated with 1% OsO_4 in 0.1 M PBS buffer for 2 h. The monolayers of cells were dried through a graded alcohol series for 10 min each, followed by a final addition of propylene oxide for 10 min. Samples were then treated with a mixture of EPON (EPON 812, MNA, DDSA, DMP30) and propylene oxide (1:1) for 18 h and heated in an embedding oven at 35℃ for 6 h, 45℃ for 12 h, and 60℃ for 24 h. The cell blocks were trimmed and sectioned at 0.25 μm using an ultramicrotome (Leica Ultracut UCT, Leica Microsystems GmbH, Wetzlar, Germany). These ultra-thin sections were stained with 1% toluidine blue and put on a

copper grid. The samples were then stained with uranyl acetate (6%) and lead citrate and analyzed using a TEM (JEM-1011, JEOL, Tokyo, Japan).

2.1.9. RNA isolation and cDNA microarray analysis

 Total RNA was extracted using the RNeasy® Mini Kit (Qiagen, Hilden, Germany) according to the manufacturer's guidelines. RNA quantity was measured using a Nanodrop ND-1000 spectrophotometer (Wilmington, DE, USA), and an RNA 260/280 ratio of 1.8-2.1 was used for all samples. Whole genome microarray analysis was performed using an Affymetrix GeneChip® Human Gene 2.0 ST Array (Affymetrix, CA, USA). This array can analyze the transcription of 24,838 RefSeq (Entrez) genes. EA.hy926 cells were plated on 60-mm Petri dishes (4.5 × 10^5 cells) overnight and then exposed to 1.5-2 μg/mL of 5 nm or 100 nm silver NPs for 6 h. cDNA was synthesized from 3 μg of total RNA in the presence of a random primer. *In vitro* transcription reactions were performed with a mixture of biotin-labeled ribonucleotides to create biotinylated cRNAs from the cDNA templates. Fluorescence intensities captured using an Affymetrix GeneChip® Scanner 3000 7G were extracted using the Affymetrix GeneChip® Command Console® Software (AGCC), converted to an absolute fold change scale, and standardized and normalized using the Robust Multi-array Average (RMA) algorithm, which normalizes the distribution of probe

intensities for all gene arrays in a given set. Gene expression values were median-centered and imported into the Expression Console 1.4 software. Principal component analysis was performed to verify the consistency of the experiments in order to determine if there were any chip outliers. Transcripts with a 1.5-fold or higher change in their expression values were selected, and a t-test was used to evaluate the significance of differences (p < 0.05).

Table 1. GeneChip® Human Gene 2.0 ST Array Specifications

Transcript coverage of the array	
NM - RefSeq coding transcript, well-established annotation	30,654
NR - RefSeq non-coding transcript, well-established annotation	5,638
XM - RefSeq coding transcript, provisional annotation	996
XR - RefSeq non-coding transcript, provisional annotation	3,428
Total RefSeq transcripts	40,716
RefSeq (Entrez) gene count	24,838
lincRNA transcripts[1]	11,086

[1] Derived from the Broad Institute's Human Body Map lincRNAs and TUCP (transcripts of uncertain coding potential) catalog and lncRNA db

2.1.10. Statistical analysis

Data are expressed as the mean ± SD. The statistical comparisons were performed using one-way ANOVA for two groups and two-way ANOVA with Bonferroni post-tests for more than two groups. Statistical analyses were performed using GraphPad Prism 5 (GraphPad Software, CA, USA). cDNA microarray results were analyzed using independent t-tests. A p-value < 0.05 was considered significant.

2.2. Effects of silver NPs on bronchial epithelial cells (BEAS-2B)

2.2.1. Cell lines and culture

  The human bronchial epithelial cell line, BEAS-2B (ATCC, Manassas, VA, USA), was isolated from normal human bronchial epithelium obtained from autopsy of non-cancerous individuals. BEAS-2B cells were cultured in Minimum Essential Medium (MEM; Welgenen, Gyeongsan, Korea) containing 10% FBS and penicillin-streptomycin (100 U/mL and 100 μg/mL, respectively) at 37℃ in a humidified 5% CO_2 incubator. Fresh culture media was added every two to three days. Although endotoxins were not detected in the silver NPs used in this study, polymyxin B at a concentration of 10 ng/mL was added as an endotoxin neutralizer.

2.2.2. Analysis of cell proliferation

  Cell viability was assessed using the CCK-8 kit. Cells were plated in 24-well plates at a density of 6×10^4 cells in 500 μL of growth medium per well and incubated overnight in a 5% CO_2 incubator. The medium was then removed and the cells were treated with 500 μL of silver NP solution diluted in 2% FBS growth medium. After 24 h, 15 μL of CCK-8 reagent was added to each well and then incubated at 37℃ for 2 h. After 13,000 rpm, 5 min centrifugation, 100 μL of supernatant was transferred to 96-

well microtiter plates and the O.D was measured at 450 nm with a spectrophotometer to ensure that there was no optical interference by silver NPs.

2.2.3. Cytokine detection

BEAS−2B cells were plated in 6−well plates at a density of 2×10^5 cells per well in 2 mL of MEM containing 10% FBS. The medium was then removed and silver NPs in 2% FBS growth medium were added to each well, to achieve a final volume of 1 mL per well. These wells were incubated for 8 h (IL−8 assay) and 24 h (IL−11 assay). After 8 h, the cell culture supernatant was collected and stored at −80℃ and the ELISA was performed using a human cytokine IL−8 assay kit. After 24 h, the cell culture supernatant was collected and stored at −80℃ and the ELISA was performed using a human cytokine IL−11 assay kit. These kits use biotinylated anti−IL−8 or anti−IL−11 detection antibodies and streptavidin conjugated to horseradish−peroxidase. The OD was measured at 450 nm.

2.2.4 Real−time RT−PCR

cDNA was synthesized from total RNA via reverse transcription with random primers. Primer pairs designed to amplify the cDNA encoding target genes were prepared using the Invitrogen Oligo Perfect Designer.

2 4

PCR reactions were performed using FastStart Universal SYBR Green Master (ROX) reagent according to the manufacturer's instructions in a 7500 and StepOne Plus Real-time PCR system.

2.2.5. Western blot

For western blot analysis, 3.5×10^5 BEAS-2B cells were seeded into 60-mm Petri dishes. The cell lysates were centrifuged at 13,000 rpm for 15 min at 4℃ and, the supernatant was stored at -20℃. The protein concentrations of the lysates were measured using the Bradford assay. From each sample, 30-40 ㎍ of protein was boiled for 5 min and loaded on a 12% SDS-polyacrylamide gel. After electrophoresis, proteins were transferred onto nitrocellulose membranes (Amersham, Glattbrugg, Switzerland). After blocking with 5% skim milk, the membranes were reacted with primary antibodies such as anti-HO-1 and anti-HSP-70 at 1:1000 dilution in 5% BSA at 4℃ overnight. After washing, the membranes were further reacted with secondary antibody (Goat Anti-Rabbit IgG; Jackson ImmunoResearch, PA, USA) at 1:2000 dilution in 5% skim milk at room temperature for 1 h. An antibody to the housekeeping gene GAPDH was used as an internal control.

2.2.6. RNA isolation and cDNA microarray analysis

Total RNA was extracted using the RNeasy® Mini Kit (Qiagen, Hilden, Germany) according to the manufacturer's guidelines. Whole genome microarray analysis was performed using an Affymetrix GeneChip® Human Gene 2.0 ST Array. BEAS-2B cells were plated on 60-mm Petri dishes (3.5×10^5 cells) overnight and then exposed to 0.5 μg/mL of 5 nm or 100 nm silver NPs for 6 h. cDNA was then synthesized from 3 μg of total RNA in the presence of a random primer. Transcripts with a 2-fold or higher change in their expression values were selected for further analysis.

3. Results

3.1 Characterization of silver NPs

Characterization of the silver NPs used in this experiment is shown in Figure 1. The size of the silver NPs was determined using TEM. The 5 nm silver NPs were comparatively consistent in size, but the size of the 100 nm silver NPs varied. Particle shape was round (Figure 1A). Dynamic light scattering (DLS) analysis showed that the hydrodynamic diameter of silver NPs was 5.3 nm for the 5 nm silver NPs and 74.2 nm for the 100 nm silver NPs (Figure 1B). DLS analysis of the size distribution of the silver NPs in DMEM medium containing 10% FBS produced a bell-shaped curve. Silver NPs were suspended in 10% FBS growth medium and 2% FBS growth medium for use with endothelial cells (EA.hy926) and epithelial cells (BEAS-2B), respectively. Silver NPs in the growth medium retained excellent dispersion and stability, and were thus suitable for further experimentation.

When spectrophotometric data are collected in nanomaterial experiments such as CCK-8 and ELISA assays, it must be verified that the NPs do not hinder the absorbance of the indicator system. Silver NPs can influence the optical density at high concentrations, and have a lesser effect at low concentrations (Figure 2). Therefore, optical density results must be corrected using a silver-NP-only sample.
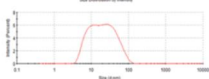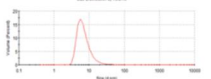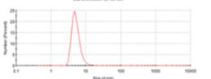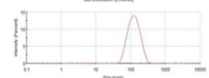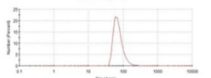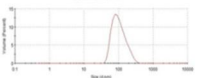
Figure 1. Analysis of silver NPs. (A) TEM images of silver NPs showed 5 nm silver NPs are relatively uniform in sizes, but, 100 nm silver NPs showed a range of different sized particles. (B) DLS analysis showed that the mean size of the 5 nm silver NPs was 5.3 nm and that of the 100 nm NPs was 74.2 nm. Silver NPs were dispersed in DMEM medium containing 10% FBS for DLS.
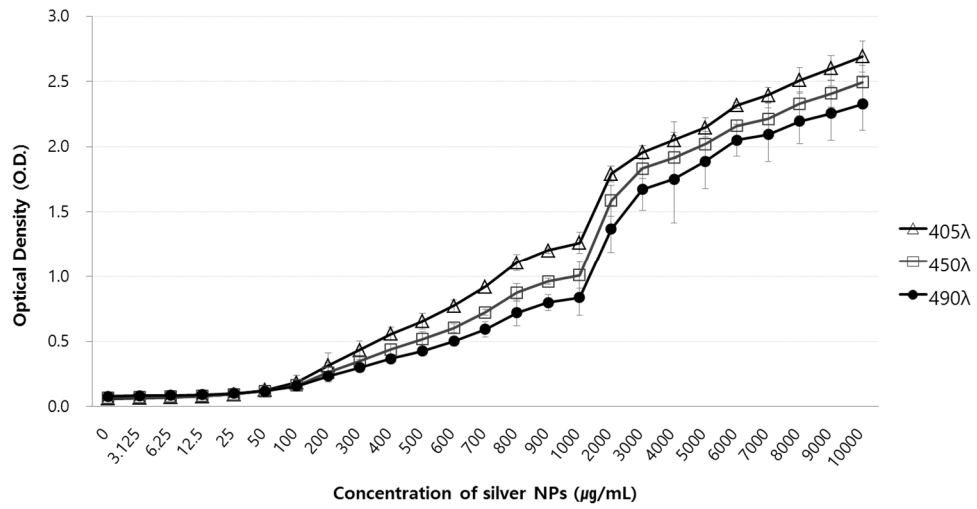
Figure 2. Influence of silver NPs on spectrophotometric analysis. Silver NPs (5 nm) were serially diluted in cell culture medium and the optical density was assessed at 405, 450, 490 nm, respectively.

3.2. Effects of silver NPs on endothelial cells

3.2.1. Cytotoxicity in endothelial cells

Viability assays are an essential step in toxicology that reveals the cellular reaction to a potential toxicant. In the present study, endothelial cells (EA.hy926) were treated with silver NPs for 24 h and cell viability was determined using a CCK-8 assay. As shown in Figure 3, cell viability decreased as the concentration of 5 nm silver NPs increased. At concentrations of 1, 1.5, 2, 2.5, 2.75, 3, and 3.5 μg/mL, cell viability was reduced to 91%, 69%, 26%, 8%, 4%, 3%, and 1%, respectively; viability was significantly lower than the control. The LD_{50} of the 5 nm silver NPs was approximately 1.72 μg/mL. However, the 100 nm silver NPs did not show cytotoxicity at up to 3.5 μg/mL (Figure 3). These results showed the toxicity of silver NPs to EA.hy926 is size and dose-dependent.
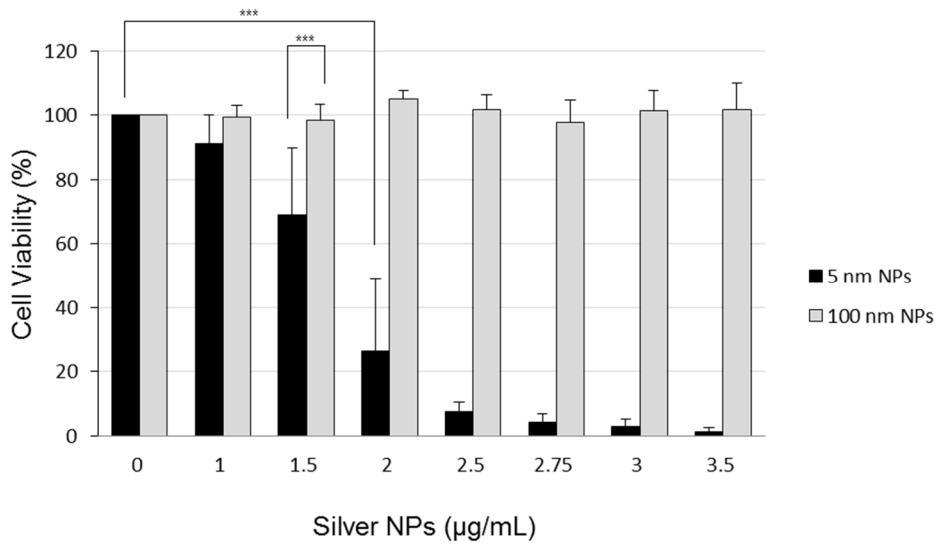
Figure 3. Cytotoxicity of silver NPs to endothelial cells. EA.hy926 cells were treated with 5 nm or 100 nm silver NPs for 24 h, and cytotoxicity was determined using a CCK−8 assay. The LD_{50} of the 5 nm silver NPs was approximately 1.72 μg/mL. Data represent the mean ± SD of three independent experiments. One−way and two−way ANOVAs were used to determine significance (***p < 0.001).

3.2.2. cDNA microarray analysis

Microarray analysis was used to detect changes in gene expression. cDNA for microarray analysis was collected after 6 h of exposure to silver NPs at near the LD_{50} concentration, in order to detect changes in gene expression at a dose that does not produce obvious cell damage. In this study, the Affymetrix GeneChip® Human Gene 2.0 ST Array was used. It is capable of analyzing 24,838 RefSeq (Entrez) genes with a total of 40,716 RefSeq transcripts. Microarray data are expressed as absolute fold change values, where each unit indicates a 1.5-fold change in expression level. Table 2 shows a summary of the differentially expressed gene (DEG) count data at 6 h post-silver NP exposure. In the DEG summary data, a 1.5-fold increase is equivalent to a doubling of expression and a 1.5-fold decrease is equivalent to a halving of expression. The Venn diagram shows that 466 genes differed in positive expression between cells exposed to 5 nm silver NPs and controls, 27 genes differed in positive expression between cells exposed to 100 nm silver NPs and controls, and 479 genes differed in positive expression between cells exposed to 100 nm silver NPs and 5 nm silver NPs (Figure 4). Selected genes with a positive absolute fold change of 2.0 or greater in 5 nm silver NP-treated cells include those associated with oxidative stress and cytokine production (Table 3). As shown in Table 3A, the gene with the highest fold change (47.9-fold) was metallothionein 1G. Heme oxygenase (decycling) 1 and heat shock 70 kDa protein 1B showed 13.3-fold and 5.1-fold changes in expression,

respectively, which were significantly higher than the control. Additionally, as shown in Table 3B, which compares gene expression between cells exposed to 100 nm and 5 nm NPs, metallothionein 1G showed the highest fold change (44.3-fold). Furthermore, heme oxygenase (decycling) 1 and heat shock 70 kDa protein 6 (HSP70B) showed 11.5-fold and 5.2-fold changes in expression, respectively, which were significantly higher than expression induced by 100 nm silver NPs. Another interesting finding is that IL-11 expression was increased 10.4-fold. Although IL-8, IL-36α and IL-1α also increased 6.1-fold 4.6-fold and 2.6-fold, respectively, the change in expression of IL-11 was the most prominent (Table 3A). The absolute fold change of IL-11 was 11.0-fold between the 100 nm silver NPs and 5 nm silver NPs treatments. However, treatment with 5 nm silver NPs did not changed expression of IL-11 receptor (IL11RA) and CXCR1 by -1.0-fold and -1.1-fold, respectively. Significantly changed interleukin receptors were IL1RL1, IL7R and IL13RA2 (Table 4). Figure 5 shows a heat map for the results for IL-11, HSP70, MT1G, and HO-1 based on the microarray results. Genes were filtered for absolute fold change > 1.5. Red indicates high expression and green indicates low expression.

Table 2. DEG (Differentially Expressed Gene) summary

Group	Up-regulation	Down-regulation	Total genes
control vs. 5 nm	466	193	659
control vs. 100 nm	27	20	47
100 nm vs. 5 nm	479	181	660

Notes: Significant transcripts were selected when expression values changed by 1.5-fold or greater and while using a t-test with p-value < 0.05.

Control v.s. 5 nm
(466 genes)

96

3   367

0

Control v.s. 100 nm   18   6   107   100 nm v.s. 5 nm
(27 genes)   (479 genes)
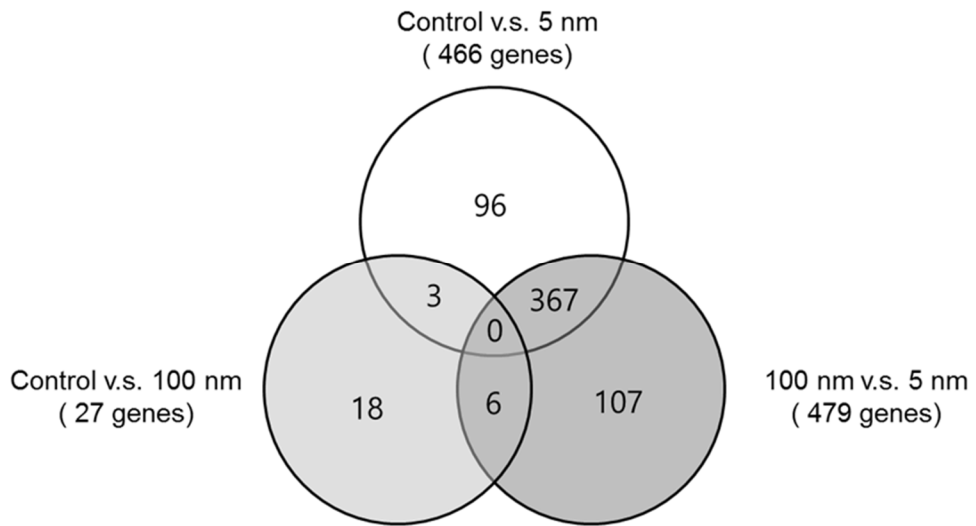
Figure 4. Microarray analysis to determine expression changes in genes. The Venn diagram shows the number of genes with increased expression after exposure to silver NPs at approximately LD_{50} for 6 h at 2 μg/mL. Data from the Affymetrix GeneChip® include 24,838 RefSeq (Entrez) genes, and are presented on an absolute fold change scale, where each unit represents a 1.5-fold change in expression level. Results were analyzed using a t-test and significance was set at p < 0.05.

Table 3. List of increased genes after silver NPs exposure

(A) Control vs. 5 nm

Genes	Fold Change	p-value
metallothionein 1G	47.9	0.0008
long intergenic non-protein coding RNA 622	15.1	0.0079
heme oxygenase (decycling) 1	13.3	0.0001
putative novel transcript	11.3	0.0189
interleukin 11	10.4	0.0015
matrix metallopeptidase 10 (stromelysin 2)	8.7	0.0040
chemokine (C-X-C motif) ligand 8	6.1	0.0045
heat shock 70kDa protein 1B	5.1	0.0004
heat shock 70kDa protein 6 (HSP70B)	4.8	0.0027
metallothionein 1E	4.6	0.0008
"interleukin 36, alpha "	4.6	0.0292
heat shock 70kDa protein 1A	4.0	0.0006
"interleukin 13 receptor, alpha 2 "	3.8	0.0474
heat shock 70kDa protein 9 (mortalin)	3.5	0.0082
interleukin 1 receptor-like 1	3.1	0.0080
interleukin 7 receptor	2.7	0.0143
"interleukin 1, alpha "	2.6	0.0215
vascular endothelial growth factor A	2.4	0.0283
metallothionein 1X	2.3	0.0019
metallothionein 1F	2.2	0.0379

Notes: Significant transcripts were selected when expression values changed by 2-fold or greater and while using a t-test with p-value < 0.05.

(B) 100 nm vs. 5 nm

Genes	Fold Change	p-vlaue
metallothionein 1G	44.3	0.0008
long intergenic non-protein coding RNA 622	18.1	0.0061
putative novel transcript	13.8	0.0140
heme oxygenase (decycling) 1	11.5	0.0001
interleukin 11	11.0	0.0013
"nuclear receptor subfamily 4, group A, member 1 "	7.9	0.0003
matrix metallopeptidase 10 (stromelysin 2)	7.8	0.0028
chemokine (C-X-C motif) ligand 8	6.4	0.0008
heat shock 70kDa protein 6 (HSP70B)	5.2	0.0026
heat shock 70kDa protein 1B	5.0	0.0005
metallothionein 1E	4.3	0.0008
"interleukin 36, alpha "	4.0	0.0391
heat shock 70kDa protein 9 (mortalin)	3.9	0.0042
heat shock 70kDa protein 1A	3.9	0.0008
"interleukin 13 receptor, alpha 2 "	3.5	0.0479
interleukin 1 receptor-like 1	2.8	0.0108
spermine oxidase	2.8	0.0069
vascular endothelial growth factor A	2.6	0.0228
"interleukin 1, alpha "	2.6	0.0191
metallothionein 1X	2.3	0.0010

Notes: Significant transcripts were selected when expression values changed by 2-fold or greater and while using a t-test with $p < 0.05$.

Table 4. List of changed interleukin receptor genes after silver NPs exposure

Genes	Fold change	Gene description	p-value
IL1R1	1.3	interleukin 1 receptor, type I	0.1464
IL1R2	−1.0	interleukin 1 receptor, type II	0.7676
IL1RL1	3.1	interleukin 1 receptor-like 1	0.0080
IL1RL2	1.1	interleukin 1 receptor-like 2	0.3853
IL2RA	1.0	interleukin 2 receptor, alpha	0.7336
IL2RB	1.1	interleukin 2 receptor, beta	0.2867
IL2RG	1.1	interleukin 2 receptor, gamma	0.6365
IL3RA	1.1	interleukin 3 receptor, alpha (low affinity)	0.2973
IL4R	1.0	interleukin 4 receptor	0.3749
IL5RA	1.0	interleukin 5 receptor, alpha	0.4756
IL6R	1.1	interleukin 6 receptor	0.4765
IL7R	2.7	interleukin 7 receptor	0.0143
CXCR1	−1.1	chemokine (C-X-C motif) receptor 1 (interleukin-8 receptor activity)	0.3498
IL9R	−1.0	interleukin 9 receptor	0.4168
IL10RA	1.1	interleukin 10 receptor, alpha	0.2260
IL10RB	−1.4	interleukin 10 receptor, beta	0.0056
IL11RA	−1.0	interleukin 11 receptor, alpha	0.4038
IL12RB1	−1.1	interleukin 12 receptor, beta 1	0.7539
IL12RB2	−1.0	interleukin 12 receptor, beta 2	0.6158
IL13RA1	−1.0	interleukin 13 receptor, alpha 1	0.3480
IL13RA2	3.8	interleukin 13 receptor, alpha 2	0.0474
IL15RA	−1.3	interleukin 15 receptor, alpha	0.1525
IL18R1	1.2	interleukin 18 receptor 1	0.1893
IL20RA	−1.2	interleukin 20 receptor, alpha	0.2701
IL20RB	1.2	interleukin 20 receptor beta	0.1646
IL21R	1.0	interleukin 21 receptor	0.9211
IL22RA1	−1.2	interleukin 22 receptor, alpha 1	0.2303
IL22RA2	1.0	interleukin 22 receptor, alpha 2	0.8908
IL23R	1.1	interleukin 23 receptor	0.2603
IL27RA	−1.3	interleukin 27 receptor, alpha	0.0726

Notes : control vs. 5 nm
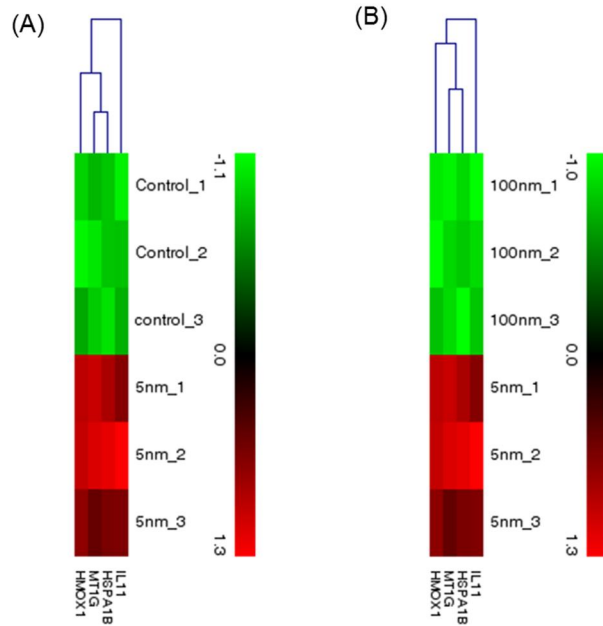
Figure 5. Hierarchical clustering. Heat map of genes showing differential expression in EA.hy926 cells based on microarray analysis. Genes were filtered for absolute fold change > 1.5. Red indicates high expression and green indicates low expression. (A) Untreated cell vs. 5 nm NP-treated cells. (B) 100 nm NP-treated cells vs. 5 nm NP-treated cells. Results were analyzed using a t-test and significance was set at p < 0.05.

3.2.3. Classification of genes that showed increased expression following treatment with silver NPs

Next, we classified the genes with an absolute fold change of 1.5 or greater, comparing the microarray results for the 5 nm silver NPs and 100 nm silver NPs. Genes were divided into five categories that showed increased gene counts based on gene ontology term: cell death (Table 5), cell survival (Table 7), inflammation (Table 11), apoptosis (Table 14), and ROS (Table 17). The cell death category includes genes involved in regulation of cell death. The number of genes regulating cell death was 37. HO-1, HSP70 and IL-1α are included herein. As shown in Table 6, HMOX1, HSPA1B and IL1A showed 13.3-fold, 5.1-fold and 2.6-fold changes in expression, respectively, which were significantly higher than the control. The cell survival category included regulation of cell proliferation, regulation of endothelial cell proliferation and regulation of vascular endothelial growth factor production. The number of genes regulating cell proliferation was 20. HO-1, IL-11 and IL-1α are included herein. As shown in Table 8, HMOX1, IL-11 and IL1A showed 13.3-fold, 10.4-fold and 2.6-fold changes in expression, respectively, which were significantly higher than the control. Also the number of genes regulating endothelial cell proliferation was 2 (Table 9). The number of genes regulating vascular endothelial growth factor production was 2. IL-1α is included herein (Table 10). The inflammation category included inflammatory response and genes involved in cytokines and inflammatory

response. The number of genes inflammatory response was 8. HO-1 and IL-1α are included herein (Table 12). In addition, the number of genes cytokines and inflammatory response was 2. IL-11 and IL-1α are included herein (Table 13). The apoptosis category included apoptotic mitochondrial changes and regulation of apoptosis. The number of genes regulation of apoptosis was 37. HO-1, HSP70 and IL-1α are included herein (Table 15). The number of genes apoptotic mitochondrial changes was 2 (Table 16). Lastly, the ROS category includes genes involved in response to oxidative stress and ion binding. The number of genes response to oxidative stress was 8. HO-1 was included herein (Table 18). The number of genes ion binding was 67. As shown in Table 19, MT1G and HMOX1 showed 47.9-fold and 13.3-fold changes in expression, respectively, which were significantly higher than the control. The high fold change of MT1G is to be due to the silver NP belongs to the metal.

In particular, IL-11 was included in the cell survival and inflammation categories. These results suggest that the 5 nm silver NPs activated inflammation and ROS, as well as stimulating expression of cell proliferation genes. Most of the stress-related genes were included in the cell death, apoptosis, and ROS categories.

Table 5. Classification of increased genes associated with cell death categories

Ontology term	Count
regulation of programmed cell death	37
regulation of cell death	37
negative regulation of programmed cell death	26
negative regulation of cell death	26
death	22
cell death	21
positive regulation of programmed cell death	12
positive regulation of cell death	12
programmed cell death	17
induction of programmed cell death	10

Notes: Significant transcripts were selected when expression values changed by 1.5-fold or greater and while using a t-test with p-value < 0.05.

Table 6. Regulation of cell death genes

Fold Change	Gene Symbol	p-value	Gene Description
13.3	HMOX1	0.0001	heme oxygenase (decycling) 1
7.9	DDIT3	0.0046	DNA-damage-inducible transcript 3
7.7	NR4A1	0.0004	"nuclear receptor subfamily 4, group A, member 1 "
5.1	HSPA1B	0.0004	heat shock 70kDa protein 1B
5.1	PTGS2	0.0279	prostaglandin-endoperoxide synthase 2 (prostaglandin G/H synthase and cyclo
4.8	HSPA1B	0.0008	heat shock 70kDa protein 1B
4.3	HSPA1B	0.0006	heat shock 70kDa protein 1B
4.0	HSPA1A	0.0006	heat shock 70kDa protein 1A
3.9	HSPA1A	0.0004	heat shock 70kDa protein 1A
3.5	HSPA9	0.0082	heat shock 70kDa protein 9 (mortalin)
3.5	HSPA1B	0.0001	heat shock 70kDa protein 1B
3.5	BAG3	0.0013	BCL2-associated athanogene 3
3.4	HSPA1A	0.0002	heat shock 70kDa protein 1A
3.4	HSPA1A	0.0002	heat shock 70kDa protein 1A
3.4	HSPA1A	0.0002	heat shock 70kDa protein 1A
3.3	HSPA1A	0.0002	heat shock 70kDa protein 1A
3.1	GCLM	0.0061	"glutamate-cysteine ligase, modifier subunit "
3.0	HERPUD1	0.0107	"homocysteine-inducible, endoplasmic reticulum stress-inducible, ubiquitin-like domain member 1 "
3.0	DEDD2	0.0482	death effector domain containing 2

2.9	NR4A2	0.0200	"nuclear receptor subfamily 4, group A, member 2 "
2.9	PMAIP1	0.0202	phorbol-12-myristate-13-acetate-induced protein 1
2.6	IL1A	0.0215	"interleukin 1, alpha "
2.6	DNAJB6	0.0062	"DnaJ (Hsp40) homolog, subfamily B, member 6 "
2.4	VEGFA	0.0283	vascular endothelial growth factor A
2.4	INHBA	0.0112	"inhibin, beta A "
2.3	CEBPB	0.0273	"CCAAT/enhancer binding protein (C/EBP), beta "
2.0	CRYAB	0.0218	"crystallin, alpha B "
2.0	SPHK1	0.0018	sphingosine kinase 1
1.8	TNFRSF10D	0.0113	"tumor necrosis factor receptor superfamily, member 10d, decoy with truncated death domain "
1.8	CEBPG	0.0359	"CCAAT/enhancer binding protein (C/EBP), gamma "
1.7	BCL2A1	0.0488	BCL2-related protein A1
1.7	F3	0.0069	"coagulation factor III (thromboplastin, tissue factor) "
1.6	DAPK3	0.0124	death-associated protein kinase 3
1.6	RB1CC1	0.0124	RB1-inducible coiled-coil 1
1.6	ABL1	0.0230	"ABL proto-oncogene 1, non-receptor tyrosine kinase "
1.6	CLU	0.0022	clusterin
1.5	SQSTM1	0.0171	sequestosome 1

Notes: Significant transcripts were selected when expression values changed by 1.5-fold or greater and while using a t-test with $p < 0.05$.

Table 7. Classification of increased genes associated with cell survival categories

Ontology term	Count
cell proliferation	10
positive regulation of cell proliferation	14
regulation of cell proliferation	20
regulation of smooth muscle cell proliferation	4
positive regulation of smooth muscle cell proliferation	3
positive regulation of endothelial cell proliferation	2
positive regulation of fibroblast proliferation	1
regulation of endothelial cell proliferation	2
regulation of fibroblast proliferation	1
negative regulation of cell proliferation	6
positive regulation vascular endothelial growth factor production	2
regulation of vascular endothelial growth factor production	2

Notes: Significant transcripts were selected when expression values changed by 1.5-fold or greater and while using a t-test with p-value < 0.05.

Table 8. Regulation of cell proliferation

Fold change	Gene Symbol	p-value	Gene Description
13.3	HMOX1	0.0001	heme oxygenase (decycling) 1
10.4	IL11	0.0015	interleukin 11
5.1	PTGS2	0.0279	prostaglandin-endoperoxide synthase 2 (prostaglandin G/H synthase and cyclooxygenase)
4.0	LIF	0.0099	leukemia inhibitory factor
3.5	ATF3	0.0228	activating transcription factor 3
2.6	IL1A	0.0215	"interleukin 1, alpha "
2.6	DDR2	0.0194	discoidin domain receptor tyrosine kinase 2
2.4	VEGFA	0.0283	vascular endothelial growth factor A
2.3	TRIB1	0.0473	tribbles pseudokinase 1
2.0	XIRP1	0.0101	xin actin-binding repeat containing 1
2.0	MAFG	0.0163	v-maf avian musculoaponeurotic fibrosarcoma oncogene homolog G
2.0	SPHK1	0.0018	sphingosine kinase 1
1.9	NOX1	0.0092	NADPH oxidase 1
1.7	VIP	0.0262	vasoactive intestinal peptide
1.7	NAMPT	0.0322	nicotinamide phosphoribosyltransferase
1.7	F3	0.0069	"coagulation factor III (thromboplastin, tissue factor) "
1.6	PROK1	0.0376	prokineticin 1
1.6	KITLG	0.0097	KIT ligand
1.6	CLU	0.0022	clusterin
1.5	WARS	0.0399	tryptophanyl-tRNA synthetase

Notes: Significant transcripts were selected when expression values changed by 1.5-fold or greater and while using a t-test with p-value < 0.05.

Table 9. Regulation of endothelial cell proliferation

Fold Change	Gene Symbol	p-value	Gene Description
2.4	VEGFA	0.0283	vascular endothelial growth factor A
1.7	F3	0.0069	"coagulation factor III (thromboplastin, tissue factor) "

Notes: Significant transcripts were selected when expression values changed by 1.5-fold or greater and while using a t-test with p-value < 0.05.

Table 10. Regulation of vascular endothelial growth factor production

Fold Change	Gene Symbol	p-value	Gene Description
2.6	IL1A	0.0215	"interleukin 1, alpha"
1.9	NOX1	0.0092	NADPH oxidase 1

Notes: Significant transcripts were selected when expression values changed by 1.5-fold or greater and while using a t-test with p-value < 0.05.

Table 11. Classification of increased genes associated with inflammation categories

Ontology term	Count
acute inflammatory response	4
inflammatory response	8
activation of plasma proteins involved in acute inflammatory response	2
Cytokines and Inflammatory Response	2

Notes: Significant transcripts were selected when expression values changed by 1.5-fold or greater and while using a t-test with p-value < 0.05.

Table 12. Inflammatory response

Fold Change	Gene Symbol	p-value	Gene Description
13.3	HMOX1	0.0001	heme oxygenase (decycling) 1
4.1	KDM6B	0.0038	lysine (K)-specific demethylase 6B
2.6	IL1A	0.0215	"interleukin 1, alpha "
2.3	CEBPB	0.0273	"CCAAT/enhancer binding protein (C/EBP), beta "
1.9	NOX1	0.0092	NADPH oxidase 1
1.7	CYP4F11	0.0292	"cytochrome P450, family 4, subfamily F, polypeptide 11 "
1.7	F3	0.0069	"coagulation factor III (thromboplastin, tissue factor) "
1.6	CLU	0.0022	clusterin

Notes: Significant transcripts were selected when expression values changed by 1.5-fold or greater and while using a t-test with p-value < 0.05.

Table 13. Cytokines and Inflammatory Response

Fold Change	Gene Symbol	p-value	Gene Description
10.4	IL11	0.0015	interleukin 11
2.6	IL1A	0.0215	"interleukin 1, alpha "

Notes: Significant transcripts were selected when expression values changed by 1.5-fold or greater and while using a t-test with p-value < 0.05.

Table 14. Classification of increased genes associated with apoptosis categories

Ontology term	Count
apoptotic nuclear changes	1
apoptotic mitochondrial changes	2
regulation of apoptosis	37
anti-apoptosis	23
negative regulation of apoptosis	26
positive regulation of apoptosis	12
apoptosis	17
induction of apoptosis	10
DNA damage response, signal transduction resulting in induction of apoptosis	2
induction of apoptosis by intracellular signals	2
Neuropeptides VIP and PACAP inhibit the apoptosis of activated T cells	2
negative regulation of neuron apoptosis	2
regulation of neuron apoptosis	2
induction of apoptosis by extracellular signals	2

Notes: Significant transcripts were selected when expression values changed by 1.5-fold or greater and while using a t-test with p-value < 0.05.

Table 15. Regulation of apoptosis

Fold Change	Gene Symbol	p-value	Gene Description
13.3	HMOX1	0.0001	heme oxygenase (decycling) 1
7.9	DDIT3	0.0046	DNA-damage-inducible transcript 3
7.7	NR4A1	0.0004	"nuclear receptor subfamily 4, group A, member 1 "
5.1	HSPA1B	0.0004	heat shock 70kDa protein 1B
5.1	PTGS2	0.0279	prostaglandin-endoperoxide synthase 2 (prostaglandin G/H synthase and cyclooxygenase)
4.8	HSPA1B	0.0008	heat shock 70kDa protein 1B
4.3	HSPA1B	0.0006	heat shock 70kDa protein 1B
4.0	HSPA1A	0.0006	heat shock 70kDa protein 1A
3.9	HSPA1A	0.0004	heat shock 70kDa protein 1A
3.5	HSPA9	0.0082	heat shock 70kDa protein 9 (mortalin)
3.5	HSPA1B	0.0001	heat shock 70kDa protein 1B
3.5	BAG3	0.0013	BCL2-associated athanogene 3
3.4	HSPA1A	0.0002	heat shock 70kDa protein 1A
3.4	HSPA1A	0.0002	heat shock 70kDa protein 1A
3.4	HSPA1A	0.0002	heat shock 70kDa protein 1A
3.3	HSPA1A	0.0002	heat shock 70kDa protein 1A
3.1	GCLM	0.0061	"glutamate-cysteine ligase, modifier subunit "
3.0	HERPUD1	0.0107	"homocysteine-inducible, endoplasmic reticulum stress-inducible, ubiquitin-like domain member 1 "
3.0	DEDD2	0.0482	death effector domain containing 2

2.9	NR4A2	0.0200	"nuclear receptor subfamily 4, group A, member 2 "
2.9	PMAIP1	0.0202	phorbol-12-myristate-13-acetate-induced protein 1
2.6	IL1A	0.0215	"interleukin 1, alpha "
2.6	DNAJB6	0.0062	"DnaJ (Hsp40) homolog, subfamily B, member 6 "
2.4	VEGFA	0.0283	vascular endothelial growth factor A
2.4	INHBA	0.0112	"inhibin, beta A "
2.3	CEBPB	0.0273	"CCAAT/enhancer binding protein (C/EBP), beta "
2.0	CRYAB	0.0218	"crystallin, alpha B "
2.0	SPHK1	0.0018	sphingosine kinase 1
1.8	TNFRSF10D	0.0113	"tumor necrosis factor receptor superfamily, member 10d, decoy with truncated death domain "
1.8	CEBPG	0.0359	"CCAAT/enhancer binding protein (C/EBP), gamma "
1.7	BCL2A1	0.0488	BCL2-related protein A1
1.7	F3	0.0069	"coagulation factor III (thromboplastin, tissue factor) "
1.6	DAPK3	0.0124	death-associated protein kinase 3
1.6	RB1CC1	0.0124	RB1-inducible coiled-coil 1
1.6	ABL1	0.0230	"ABL proto-oncogene 1, non-receptor tyrosine kinase "
1.6	CLU	0.0022	clusterin
1.5	SQSTM1	0.0171	sequestosome 1

Notes: Significant transcripts were selected when expression values changed by 1.5-fold or greater and while using a t-test with p-value < 0.05.

Table 16. Apoptotic mitochondrial changes

Fold Change	Gene Symbol	p-value	Gene Description
2.9	PMAIP1	0.0202	phorbol-12-myristate-13-acetate-induced protein 1
1.6	CLU	0.0022	clusterin

Notes: Significant transcripts were selected when expression values changed by 1.5-fold or greater and while using a t-test with p-value < 0.05.

Table 17. Classification of increased genes associated with ROS categories

Ontology term	Count
response to reactive oxygen species	3
oxygen and reactive oxygen species metabolic process	2
response to oxidative stress	8
Oxidative Stress Induced Gene Expression Via Nrf2	4
cadmium ion binding	4
transition metal ion binding	54
zinc ion binding	45
copper ion binding	4
iron ion binding	7
magnesium ion binding	8
cation binding	67
ion binding	67
metal ion binding	65
manganese ion binding	3
calcium ion binding	5

Notes: Significant transcripts were selected when expression values changed by 1.5-fold or greater and while using a t-test with p-value < 0.05.

Table 18. Response to oxidative stress

Fold Change	Gene Symbol	p-value	Gene Description
13.3	HMOX1	0.0001	heme oxygenase (decycling) 1
7.9	DDIT3	0.0046	DNA-damage-inducible transcript 3
5.1	PTGS2	0.0279	prostaglandin-endoperoxide synthase 2 (prostaglandin G/H synthase and cyclooxygenase)
3.1	GCLM	0.0061	"glutamate-cysteine ligase, modifier subunit "
2.2	SRXN1	0.0057	sulfiredoxin 1
2.1	SELK	0.0223	selenoprotein K
2.0	CRYAB	0.0218	"crystallin, alpha B "
1.6	CLU	0.0022	clusterin

Notes: Significant transcripts were selected when expression values changed by 1.5-fold or greater and while using a t-test with p-value < 0.05.

Table 19. Ion binding

Fold Change	Gene Symbol	p-value	Gene Description
47.9	MT1G	0.0008	metallothionein 1G
13.3	HMOX1	0.0001	heme oxygenase (decycling) 1
8.7	MMP10	0.0040	matrix metallopeptidase 10 (stromelysin 2)
7.7	NR4A1	0.0004	"nuclear receptor subfamily 4, group A, member 1 "
7.4	ZFAND2A	0.0001	"zinc finger, AN1-type domain 2A "
6.2	SLC30A1	0.0006	"solute carrier family 30 (zinc transporter), member 1 "
5.1	PTGS2	0.0279	prostaglandin-endoperoxide synthase 2 (prostaglandin G/H synthase and cyclooxygenase)
4.6	MT1E	0.0008	metallothionein 1E
4.6	NR4A3	0.0030	"nuclear receptor subfamily 4, group A, member 3 "
4.1	KDM6B	0.0038	lysine (K)-specific demethylase 6B
3.9	HIVEP2	0.0133	human immunodeficiency virus type I enhancer binding protein 2
3.0	SNAI1	0.0047	snail family zinc finger 1
2.9	RYBP	0.0062	RING1 and YY1 binding protein
2.9	NR4A2	0.0200	"nuclear receptor subfamily 4, group A, member 2 "
2.9	JMJD1C	0.0182	jumonji domain containing 1C
2.5	YOD1	0.0463	YOD1 deubiquitinase
2.4	TES	0.0160	testis derived transcript (3 LIM domains)

2.4	GEM	0.0050	GTP binding protein overexpressed in skeletal muscle
2.3	ZNF804A	0.0249	zinc finger protein 804A
2.3	FBXO30	0.0007	F-box protein 30
2.3	MT1X	0.0019	metallothionein 1X
2.2	MT1F	0.0379	metallothionein 1F
2.2	SRXN1	0.0057	sulfiredoxin 1
2.0	SPHK1	0.0018	sphingosine kinase 1
2.0	ZSWIM6	0.0121	"zinc finger, SWIM-type containing 6 "
1.9	ZCCHC6	0.0459	"zinc finger, CCHC domain containing 6 "
1.9	NOX1	0.0092	NADPH oxidase 1
1.9	GCM1	0.0070	glial cells missing homolog 1 (Drosophila)
1.9	SEC24A	0.0149	SEC24 family member A
1.9	ABL2	0.0015	"ABL proto-oncogene 2, non-receptor tyrosine kinase "
1.9	ENTPD7	0.0205	ectonucleoside triphosphate diphosphohydrolase 7
1.8	CRELD2	0.0419	cysteine-rich with EGF-like domains 2
1.8	RAPGEF2	0.0039	Rap guanine nucleotide exchange factor (GEF) 2
1.8	RPS6KA3	0.0266	"ribosomal protein S6 kinase, 90kDa, polypeptide 3 "
1.7	CSGALNACT2	0.0248	chondroitin sulfate N-acetylgalactosaminyltransferase 2
1.7	ZNF175	0.0287	zinc finger protein 175
1.7	GLA	0.0020	"galactosidase, alpha "
1.7	DNAJA1	0.0231	"DnaJ (Hsp40) homolog, subfamily A, member 1 "

1.7	CYP4F11	0.0292	"cytochrome P450, family 4, subfamily F, polypeptide 11 "
1.7	ZBTB43	0.0435	zinc finger and BTB domain containing 43
1.7	PGM3	0.0367	phosphoglucomutase 3
1.7	ZNF697	0.0160	zinc finger protein 697
1.7	ZNF460	0.0244	zinc finger protein 460
1.7	ZNF34	0.0055	zinc finger protein 34
1.6	EGR3	0.0026	early growth response 3
1.6	JMJD6	0.0471	jumonji domain containing 6
1.6	ME1	0.0143	"malic enzyme 1, NADP(+)-dependent, cytosolic "
1.6	ZFAND5	0.0068	"zinc finger, AN1-type domain 5 "
1.6	MBNL2	0.0004	muscleblind-like splicing regulator 2
1.6	STK38L	0.0069	serine/threonine kinase 38 like
1.6	GTF2B	0.0279	general transcription factor IIB
1.6	PPP1R10	0.0407	"protein phosphatase 1, regulatory subunit 10 "
1.6	PPP1R10	0.0407	"protein phosphatase 1, regulatory subunit 10 "
1.6	PPP1R10	0.0407	"protein phosphatase 1, regulatory subunit 10 "
1.6	PPP1R10	0.0407	"protein phosphatase 1, regulatory subunit 10 "
1.6	BRF2	0.0453	"BRF2, RNA polymerase III transcription initiation factor 50 kDa subunit "
1.6	ABL1	0.0230	"ABL proto-oncogene 1, non-receptor tyrosine kinase "
1.5	SLC3A2	0.0158	"solute carrier family 3 (amino acid transporter heavy chain), member 2 "
1.5	PAPPA2	0.0483	pappalysin 2

1.5	LOC727896	0.0003	cysteine and histidine-rich domain (CHORD) containing 1 pseudogene
1.5	PPP1R10	0.0439	"protein phosphatase 1, regulatory subunit 10 "
1.5	PPP1R10	0.0439	"protein phosphatase 1, regulatory subunit 10 "
1.5	PPP1R10	0.0439	"protein phosphatase 1, regulatory subunit 10 "
1.5	SQSTM1	0.0171	sequestosome 1
1.5	ZNF384	0.0158	zinc finger protein 384
1.5	DLL1	0.0465	delta-like 1 (Drosophila)
1.5	ZNF876P	0.0288	"zinc finger protein 876, pseudogene "

Notes: Significant transcripts were selected when expression values changed by 1.5-fold or greater and while using a t-test with p-value < 0.05.

3.2.4. Effects of silver NPs on cytokine production and the inflammatory response

EA.hy926 cells were treated with 5 nm and 100 nm silver NPs and cytokine production was assessed by ELISA. Endothelial cells were treated with different concentrations of silver NPs for 8 h (Figure 6A) and 24 h (Figure 6B). Because IL-8 is an earlier-responding cytokine, the two experiments used different treatment times. Supernatants harvested from control and silver NP-treated cells were assayed for IL-8 and IL-11. IL-8 and IL-11 was the amount expressed in a concentration of 2.5 μg/mL for 5 nm treatment group 1,000 pg/mL or more. The reason for decreased interleukin expression levels in a high concentration, because the cells are dead. As predicted, treatment with 100 nm silver NPs did not increase IL-8 or IL-11 release. Thus, expression of cytokines increased in a size- and dose-dependent manner in response to silver NPs in endothelial cells. Furthermore, these results support the results of the cDNA microarray analysis.

(A)

(B)
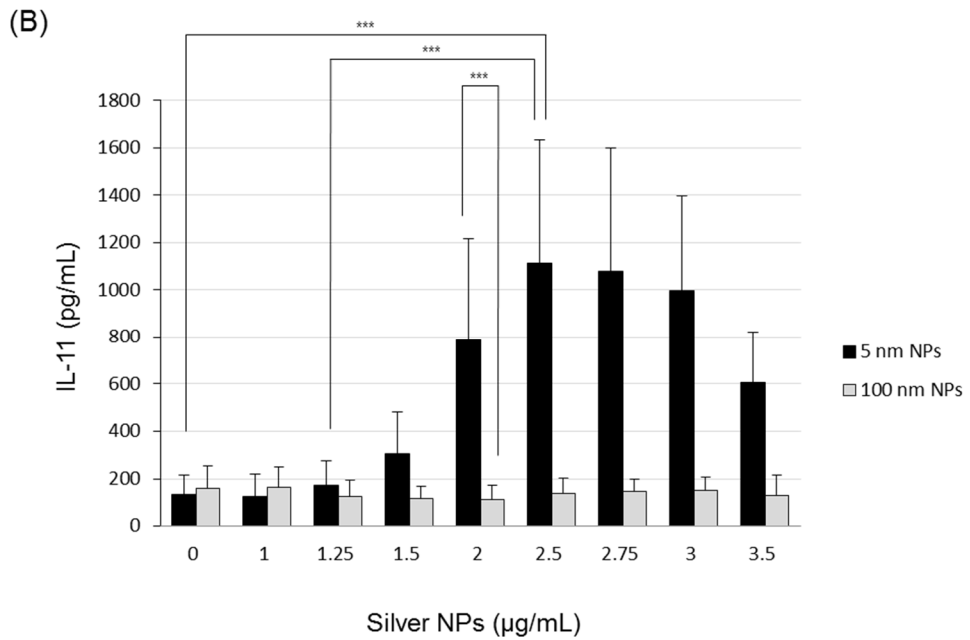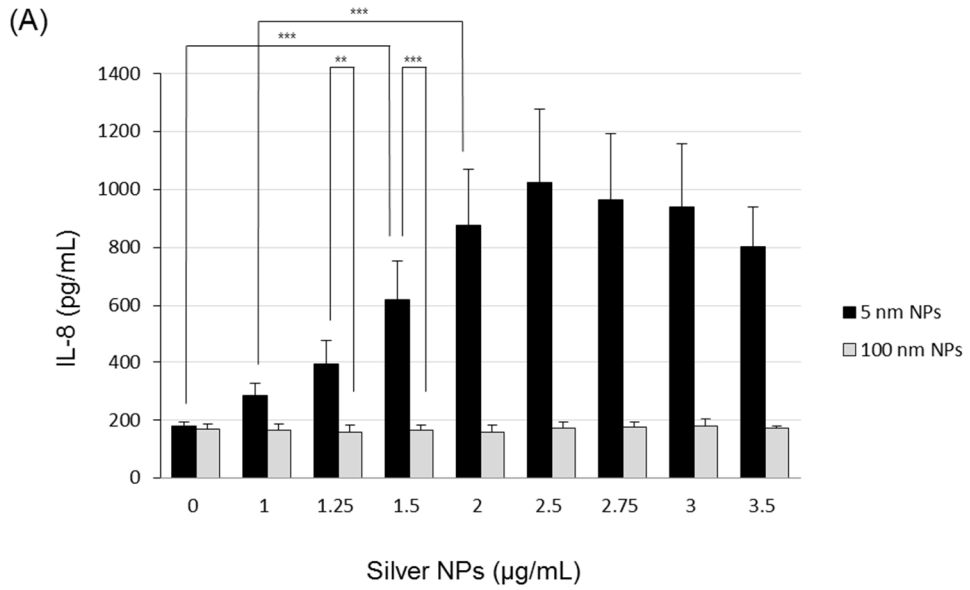
Figure 6. Dose-dependent expression of cytokines in response to silver NPs. (A) EA.hy926 cells treated with different doses of silver NPs for 8 h. (B) EA.hy926 cells treated with different doses of silver NPs for 24 h. Culture supernatant was harvested and the levels of IL-8 and IL-11 were measured by ELISA. Treatment with 5 nm silver NPs induced IL-8 and IL-11 release, but 100 nm silver NPs did not. Data represent the mean ± SD of three independent experiments. One-way and two-way ANOVA analyses were used to determine significance (**$p < 0.01$, ***$p < 0.001$).

3.2.5. Expression of genes related to cytokine production and ROS

IL-11, a gene found to be significantly increased by silver NP treatment in the cDNA microarray analysis, IL-8, HSP70 and HO-1 were included in the real-time RT-PCR analysis. Real-time RT-PCR analysis was performed after 6 h of exposure to 1.5 and 2 μg/mL of silver NPs. At concentrations of 1.5 and 2 μg/mL, IL-8 gene expression increased by 3.5- and 6.5-fold, respectively. At the same concentrations, IL-11 gene expression by 2.9- and 6.2-fold, respectively (Figure 7A). In addition, at the same doses, HSP70 gene expression increased by 3- and 27-fold, respectively. Lastly, at these concentrations, HO-1 gene expression increased by 9.8- and 19.7-fold, respectively (Figure 7B). In concordance with the microarray data, genes related to cytokine production and ROS showed increased expression after treatment with 5 nm silver NPs. However, treatment with 100 nm silver NPs did not induce increased expression of IL-8, IL-11, HSP70, or HO-1. Thus, the microarray and real-time RT-PCR data were in accord.

(A)

(B)
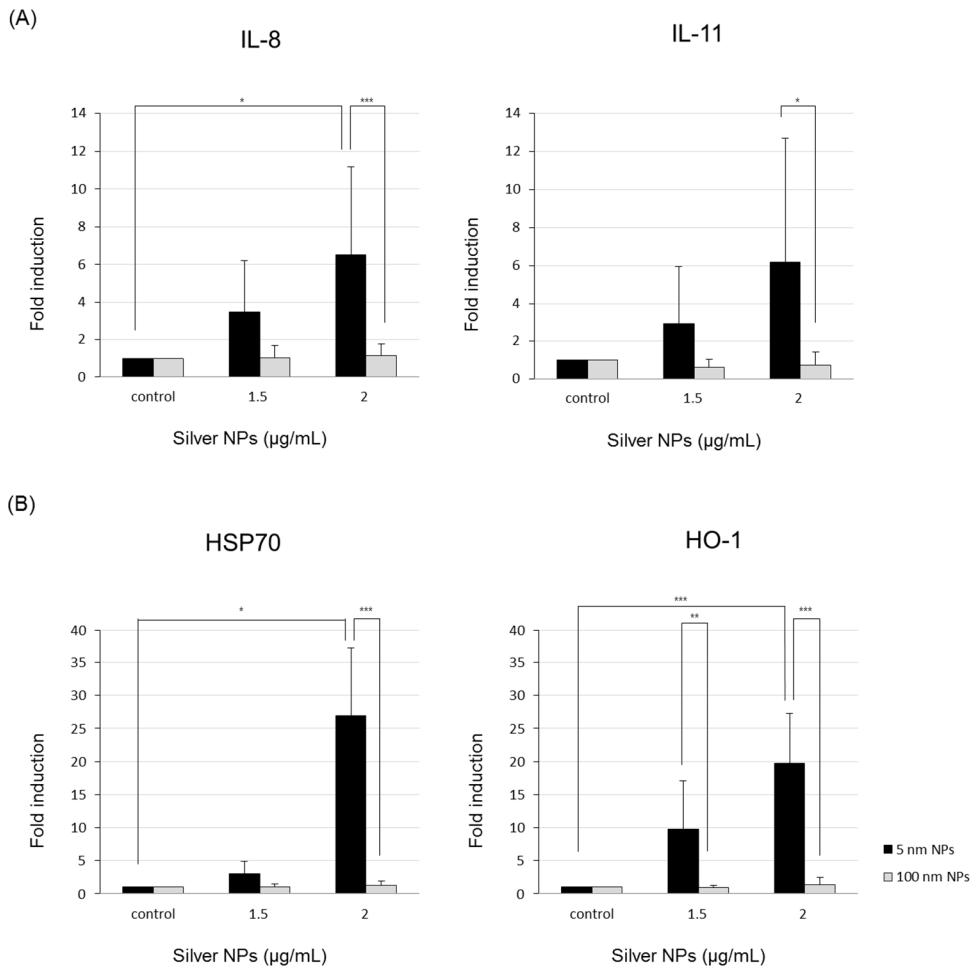
Figure 7. Expression of cytokine- and ROS-related genes in endothelial cells treated with silver NPs. (A) Real-time RT-PCR analysis was performed for 6 h at 1.5 and 2 μg/mL of silver NPs. Expression of genes related to cytokine production increased after treatment with 5 nm silver NPs, but not after treatment with 100 nm silver NPs. (B) Expression of ROS-related genes. Real-time RT-PCR analysis was performed for 6 h at 1.5 and 2 μg/mL of silver NPs. Exposure to 5 nm silver NPs induced

expression of HSP70 and HO-1. Exposure to 100 nm silver NPs did not induce the expression of HSP70 or HO-1. Real-time RT-PCR was performed three times and representative data are shown. Data are shown as the mean ± SD of three or more independent experiments. One-way and two-way ANOVA analyses were used to determine significance (*p< 0.05, **p < 0.01, ***p < 0.001).

3.2.6. Effects of silver NPs on HSP70 and HO-1 expression

For further verification, western blot analysis of two proteins (HSP70 and HO-1) was performed; the proteins were chosen based on the level of increased expression in response to treatment with 5 nm silver NPs. In accordance with the realtime-PCR results showed that RNA levels of HSP70 increased to a maximum of 27-fold and HO-1 increased to a maximum of 19.7-fold at 6 h-exposure. Therefore we tested the effect of silver NPs on the expression of HSP70 and HO-1 protein in EA.hy926 cells. EA.hy926 cells were treated with different doses of silver NPs for 24 h. Each 40-μg protein sample was loaded and analyzed using anti-HSP70, anti-HO-1, and anti-GAPDH (loading control) antibodies. HSP70 and HO-1 expression increased in cells treated with high-dose silver NPs compared to untreated cells. HSP70 protein levels increased by a maximum of 8.7-fold at 2.75 μg/mL (Figure 8A) and HO-1 protein levels increased by a maximum 33.5-fold at 3 μg/mL (Figure 8B) compared to the results for untreated cells. In contrast, ROS-associated proteins were not affected by treatment with 100 nm silver NPs. These results suggest that exposure to silver NPs could increase the expression of oxidative stress-related proteins.
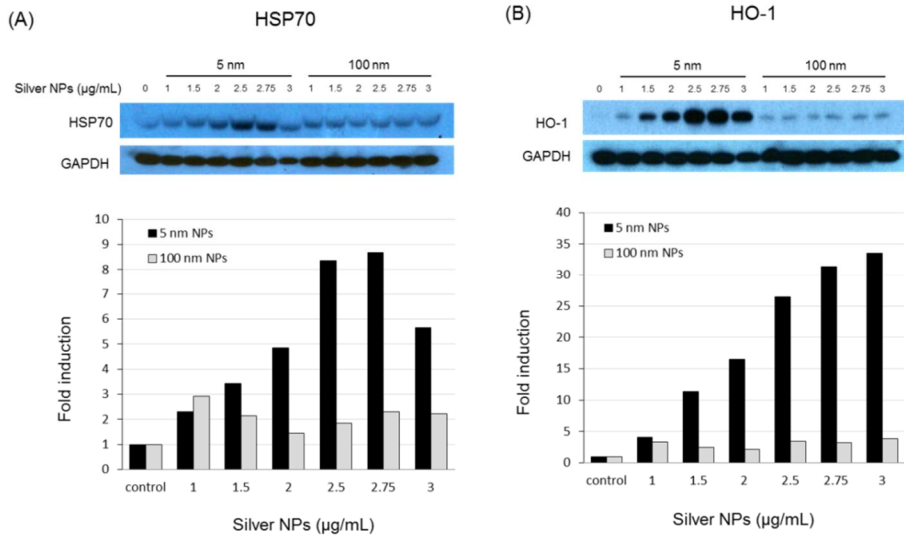
Figure 8. Protein levels of HSP70 and HO-1 in endothelial cells treated with silver NPs. EA.hy926 cells were treated with different doses of silver NPs for 24 h. Each 40-㎍ protein sample was loaded and analyzed with anti-HSP70, anti-HO-1, and anti-GAPDH (loading control) antibodies.

3.2.7. Intracellular localization of silver NPs

The transportation and localization of silver NPs in EA.hy926 cells were observed by TEM. A representative image of one EA.hy926 cell treated with 1.5 ㎍/mL silver NPs for 30 min is shown. Untreated cells showed no abnormalities, but cells treated with 5 nm silver NPs showed internalization of NPs in vesicles (black arrow). Furthermore, mitochondrial swelling, decrease or disappearance of cytoplasm, and vacuolization were observed after treatment with 5 nm silver NPs. After treatment with 100 nm silver NPs, no clear changes in cell morphology were observed, even if the presence of NPs in lysosomes and the nucleus (Figure 9).
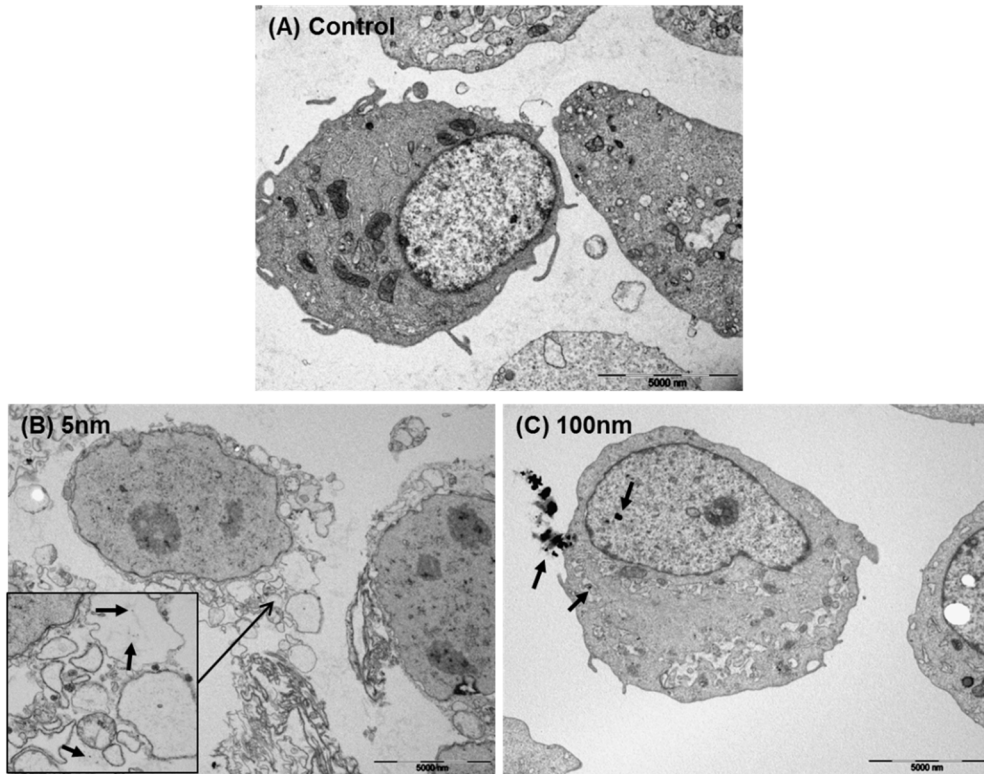
Figure 9. Transmission electron microscopy (TEM) of endothelial cells after exposure to silver NPs. Representative ultrastructural images of one EA.hy926 cell treated with 1.5 μg/mL silver NPs for 30 min. (A) Untreated cells showed no abnormalities. (B) Cells treated with 5 nm silver NPs. NPs translocated into EA.hy926 cells. NPs internalized in vesicles (black arrow) are shown. (C) Cells treated with 100 nm silver NPs. No morphological abnormalities were observed, and NPs were localized in lysosomes and the nucleus. Images shown are representatives of three independent trials.

3.3. Effects of silver NPs on bronchial epithelial cells

3.3.1. Cytotoxicity in bronchial epithelial cells

Epithelial cells (BEAS-2B) were treated with silver NPs for 24 h and cell viability was determined with the CCK-8 assay. As shown in Figure 10, cell viability decreased as the concentration of 5 nm silver NPs increased. At concentrations 0.5, 0.75, 1, 1.25, and 1.5 μg/mL, cell viability was reduced to 77%, 33%, 19%, 11%, and 5%, respectively: significantly lower than the control. The LD_{50} of 5 nm silver NPs was approximately 0.65 μg/mL. In contrast, 100 nm silver NPs did not show cytotoxicity at up to 1.5 μg/mL (Figure 10). These results showed that the toxicity of silver NPs to BEAS-2B cells is size and dose-dependent.
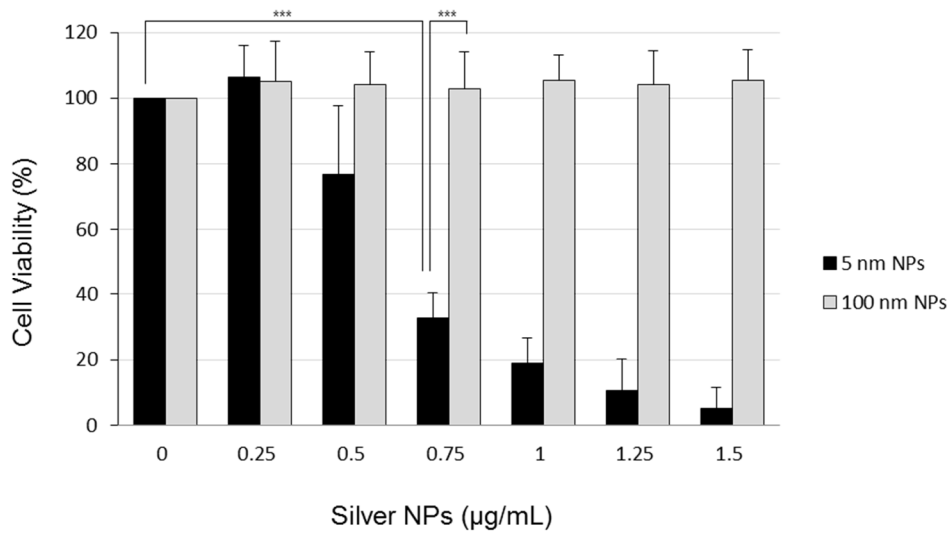
Figure 10. Cytotoxicity of silver NPs in bronchial epithelial cells. BEAS-2B cells were treated with 5 nm or 100 nm silver NPs for 24 h, and cytotoxicity was determined with the CCK-8 assay. The LD_{50} of 5 nm silver NPs was approximately 0.65 ㎍/mL. Data represent the mean ± SD of three independent experiments. One-way and two-way ANOVA analyses were used to determine significance (***p < 0.001).

3.3.2. cDNA microarray analysis

Microarray analysis was used to detect changes in gene expression. cDNA for microarray analysis was collected after 6 h of exposure to silver NPs at 0.5 μg/mL to determine changes in gene expression that occur at a dose that does not produce obvious cell damage. In this study, the Affymetrix GeneChip® Human Gene 2.0 ST Array was used. Microarray data were assigned an absolute fold change value, where each unit indicates a 2-fold change in expression level. Table 20 shows DEG counts summary data after 6 h of silver NP exposure. DEG summary data are shown as numerical values for which a 2-fold increase is equivalent to a doubling of expression and a 2-fold decrease, to a halving of expression. The Venn diagram shows that 718 genes showed differences in expression between the control and 5 nm silver NP treatments, 26 genes differed between the control and 100 nm silver NP treatments, and 787 genes differed between the 100 nm silver NP and 5 nm silver NP treatments. The increased expressed gene in common in the three groups is three, which is the MT1E, MT1B and solute carrier family30 (zinc transporter) member 1 (Figure 11). Genes with greater than 2-fold positive change in their absolute expression levels include those associated with oxidative stress and cytokine production in cells treated with 5 nm silver NPs (Table 21). As shown in Table 21 (A), the activity-regulated cytoskeleton-associated protein showed the highest fold change (46.1-fold). The levels of the heat shock 70 kDa protein 7, heme oxygenase (decycling) 1, and metallothionein

7 3

1B were 36.4-fold, 18.1-fold, and 12.8-fold higher than those in the controls, respectively; which were significantly higher than the control. Additionally, as shown in Table 21 (B), which compares gene expression between cells exposed to 100 nm and 5 nm NPs, activity-regulated cytoskeleton-associated protein showed the highest fold change (48.0-fold). In addition, the expression levels of the heat shock 70 kDa protein 7, heme oxygenase (decycling) 1, and metallothionein 1G were 28.9-fold, 12.6-fold and 6.0-fold increased, respectively. These genes showed higher expression in cells treated with 5 nm silver NPs than in cells treated with 100 nm silver NPs. Another interesting finding is that IL-8 and IL-11 expression were increased 9.8-fold and 6.2-fold, respectively (Table 21 (A)). IL-8 and IL-11 showed 11.5-fold and 6.0-fold differences in expression between 100 nm silver NP and 5 nm silver NP-treatments. However, treatment with 5 nm silver NPs did not changed expression of IL-11 receptor (IL11RA) and CXCR1 by -1.2-fold and 1.1-fold, respectively. Significantly changed interleukin receptors were IL1RL1 and IL6R (Table 22). Changes in the expression of IL-8, IL-11, heat shock protein 70 kDa, metallothionein 1G, and heme oxygenase (decycling) 1, based on microarray results, are shown as a heat map (Figure 12). Genes were filtered for absolute fold change > 2. Red indicates high expression and green indicates low expression.

Table 20. DEG (Differentially Expressed Gene) summary

Group	Up-regulation	Down-regulation	Total genes
control vs. 5 nm	726	242	968
control vs. 100 nm	39	55	94
100 nm vs. 5 nm	821	251	1,072

Notes: Significant transcripts were selected when expression values changed by 2-fold.
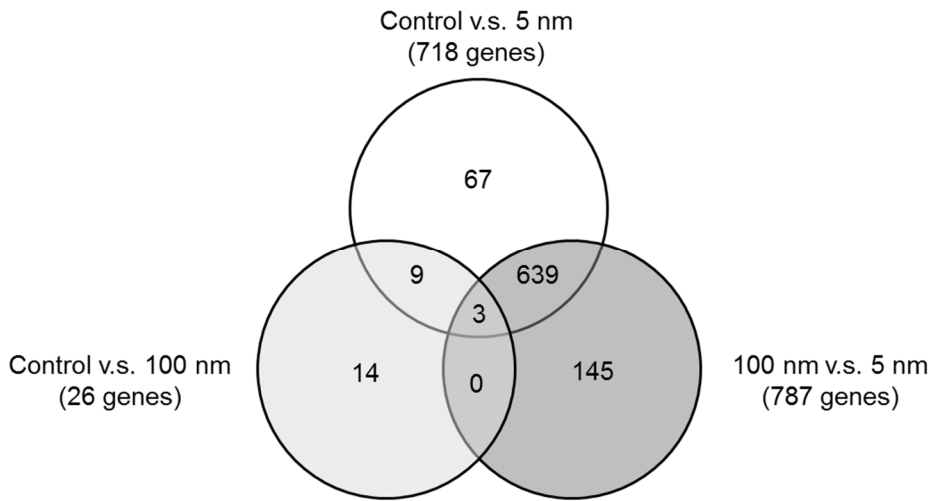
Figure 11. Microarray analysis to determine changes in expression of genes. Venn diagram showing the number of genes with increased expression after exposure to 0.5 μg/mL silver NPs for 6 h. Data from the Affymetrix GeneChip® includes 24,838 RefSeq (Entrez) genes, and is presented on an absolute fold change scale, where each unit represents a 2-fold change in expression level.

Table 21. List of increased genes after silver NPs exposure

(A) Control vs. 5 nm

Genes	Fold Change
activity-regulated cytoskeleton-associated protein	46.1
heat shock 70kDa protein 7 (HSP70B)	36.4
heme oxygenase (decycling) 1	18.1
metallothionein 1B	12.8
metallothionein 1E	12.7
heat shock 70kDa protein 6 (HSP70B')	11.1
interleukin 8	9.8
metallothionein 1G	6.8
interleukin 11	6.2
interleukin 1 receptor-like 1	5.4
metallothionein 1M	5.1
heat shock 70kDa protein 1B	4.2
BCL2-associated athanogene 3	3.7
heat shock 70kDa protein 1A	3.5
cytochrome P450, family 4, subfamily F, polypeptide 11	3.4
heat shock 70kDa protein 9 (mortalin)	3.4
VGF nerve growth factor inducible	3.1
oxidative stress responsive serine-rich 1	2.7
heparin-binding EGF-like growth factor	2.6
Smad nuclear interacting protein 1	2.4

Notes: Significant transcripts were selected when expression values changed by 2-fold.

(B) 100 nm vs. 5 nm

Genes	Fold Change
activity-regulated cytoskeleton-associated protein	48.0
heat shock 70kDa protein 7 (HSP70B)	28.9
heme oxygenase (decycling) 1	12.6
interleukin 8	11.5
heat shock 70kDa protein 6 (HSP70B')	9.9
metallothionein 1G	6.0
interleukin 11	6.0
metallothionein 1B	5.4
interleukin 1 receptor-like 1	5.4
metallothionein 1E	4.7
heat shock 70kDa protein 1-like	4.5
heat shock 70kDa protein 1B	4.4
metallothionein 1M	3.8
heat shock 70kDa protein 9 (mortalin)	3.7
BCL2-associated athanogene 3	3.6
heat shock 70kDa protein 1A	3.4
VGF nerve growth factor inducible	3.1
BCL2-related protein A1	2.4
interleukin 6 receptor	2.2
heat shock 22kDa protein 8	2.1

Notes: Significant transcripts were selected when expression values changed by 2-fold.

Table 22. List of changed interleukin receptor genes after silver NPs exposure

Genes	Fold change	Gene description
IL1R1	1.2	interleukin 1 receptor, type I
IL1R2	1.0	interleukin 1 receptor, type II
IL1RL1	5.4	interleukin 1 receptor-like 1
IL1RL2	1.0	interleukin 1 receptor-like 2
IL2RA	1.0	interleukin 2 receptor, alpha
IL2RB	1.0	interleukin 2 receptor, beta
IL2RG	1.0	interleukin 2 receptor, gamma
IL3RA	1.0	interleukin 3 receptor, alpha (low affinity)
IL4R	1.9	interleukin 4 receptor
IL5RA	1.0	interleukin 5 receptor, alpha
IL6R	2.2	interleukin 6 receptor
IL7R	1.0	interleukin 7 receptor
CXCR1	1.1	chemokine (C-X-C motif) receptor 1 (interleukin-8 receptor activity)
IL9R	1.0	interleukin 9 receptor
IL10RA	1.6	interleukin 10 receptor, alpha
IL10RB	-1.4	interleukin 10 receptor, beta
IL11RA	-1.2	interleukin 11 receptor, alpha
IL12RB1	1.0	interleukin 12 receptor, beta 1
IL12RB2	1.0	interleukin 12 receptor, beta 2
IL13RA1	1.0	interleukin 13 receptor, alpha 1
IL13RA2	1.2	interleukin 13 receptor, alpha 2
IL15RA	1.0	interleukin 15 receptor, alpha
IL18R1	1.0	interleukin 18 receptor 1
IL20RA	1.0	interleukin 20 receptor, alpha
IL20RB	1.0	interleukin 20 receptor beta
IL21R	1.0	interleukin 21 receptor
IL22RA1	-1.1	interleukin 22 receptor, alpha 1
IL22RA2	1.0	interleukin 22 receptor, alpha 2
IL23R	1.0	interleukin 23 receptor
IL27RA	1.0	interleukin 27 receptor, alpha

Notes : control vs. 5 nm
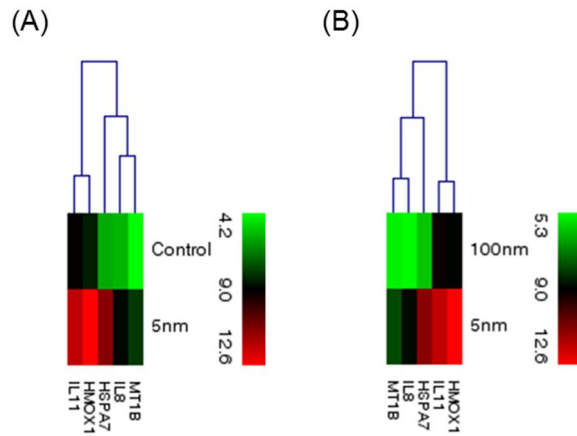
Figure 12. Hierarchical clustering. Heat map of genes showing microarray-based differential expression in BEAS-2B cells. Genes were filtered for absolute fold change > 2. Red indicates high expression and green indicates low expression. (A) Control vs. cells treated with 5 nm NPs. (B) Cells treated with 100 nm NPs vs. cells treated with 5 nm NPs.

3.3.3. Classification of genes that showed increased expression following treatment with silver NPs

Next, we classified the genes that showed an absolute fold change of 2.0 or greater, based on the microarray analysis of cells treated with 5 nm silver NPs and 100 nm silver NPs. Genes were divided into five categories based on gene ontology term: cell death (Table 23), cell survival (Table 25), inflammation (Table 28), apoptosis (Table 31), and ROS (Table 34). The cell death category includes genes involved in regulation of cell death. The number of genes regulating cell death was 49. HO-1 and HSP70 are included herein. As shown in Table 24, HMOX1 and HSPA1B showed 18.1-fold and 4.2-fold changes in expression, respectively, which were significantly higher than the control. The cell survival category includes genes involved in regulation of cell proliferation and regulation of epithelial cell proliferation. The number of genes regulating cell proliferation was 31. HO-1, IL-8 and IL-11 are included herein. As shown in Table 26, HMOX1, IL8 and IL11 showed 18.1-fold, 9.8-fold and 6.2-fold changes in expression, respectively, which were significantly higher than the control. Also the number of genes regulating epithelial cell proliferation was 3 (Table 27). The inflammation category included inflammatory response and genes involved in cytokines and inflammatory response. The number of genes inflammatory response was 16. HO-1 and IL-8 are included herein (Table 29). In addition, the number of genes cytokines and inflammatory response was 3. IL-8 and IL-11 are included herein (Table 30). The

apoptosis category included regulation of apoptosis and apoptotic mitochondrial changes. The number of genes regulation of apoptosis was 49. HO−1 and HSP70 are included herein (Table 32). The number genes apoptotic mitochondrial changes was 3 (Table 33). Lastly, the ROS−related category includes genes involved in response to oxidative stress and ion binding. The number of genes response to oxidative stress was 11. HO−1 was included herein (Table 35). The number of genes ion binding was 74. As shown in Table 36, HMOX1 and MT1 showed 18.1−fold and 12.8−fold changes in expression, respectively, which were significantly higher than the control. The high fold change of MT1 is to be due to the silver NP belongs to the metal.

In particular, IL−11 was included in the cell survival and inflammation categories. These results suggest that exposure to the 5 nm silver NPs activated genes involved in inflammation and ROS, as well as those involved in cell proliferation. Most of the stress−related genes were included in the cell death, apoptosis, and ROS categories.

Table 23. Classification of increased genes associated with cell death categories

Ontology term	Count
regulation of cell death	49
regulation of programmed cell death	49
negative regulation of programmed cell death	36
negative regulation of cell death	36
death	28
cell death	27
programmed cell death	26
positive regulation of cell death	17
positive regulation of programmed cell death	17
induction of programmed cell death	11

Notes: Significant transcripts were selected when expression values changed by 2-fold.

Table 24. Regulation of cell death genes

Fold Change	Gene Symbol	Gene Description
18.1	HMOX1	heme oxygenase (decycling) 1
10.6	NR4A1	"nuclear receptor subfamily 4, group A, member 1 "
9.7	DDIT3	DNA-damage-inducible transcript 3
4.9	SERPINB2	"serpin peptidase inhibitor, clade B (ovalbumin), member 2 "
4.5	KLF10	Kruppel-like factor 10
4.5	PMAIP1	phorbol-12-myristate-13-acetate-induced protein 1
4.4	DUSP1	dual specificity phosphatase 1
4.2	HSPA1B	heat shock 70kDa protein 1B
4.1	PIM1	pim-1 oncogene
4.0	HSPA1B	heat shock 70kDa protein 1B
4.0	HSPA1B	heat shock 70kDa protein 1B
3.9	DDIT3	DNA-damage-inducible transcript 3
3.7	UBC	ubiquitin C
3.7	BAG3	BCL2-associated athanogene 3
3.7	HSPA1B	heat shock 70kDa protein 1B
3.6	CRYAB	"crystallin, alpha B "
3.5	HSPA1B	heat shock 70kDa protein 1B // heat shock 70kDa protein 1A
3.5	HSPA1A	heat shock 70kDa protein 1A
3.4	ROCK1P1	"Rho-associated, coiled-coil containing protein kinase 1 pseudogene 1 "
3.4	HSPA9	heat shock 70kDa protein 9 (mortalin)
3.2	ANGPTL4	angiopoietin-like 4
3.2	JUN	jun proto-oncogene
3.2	HSPA1A	heat shock 70kDa protein 1A
3.2	ERN1	endoplasmic reticulum to nucleus signaling 1

3.1	HSPA1A	heat shock 70kDa protein 1A
3.1	HSPA1A	heat shock 70kDa protein 1A
3.1	HSPA1A	heat shock 70kDa protein 1A
3.1	HRK	"harakiri, BCL2 interacting protein (contains only BH3 domain) "
3.0	NR4A2	"nuclear receptor subfamily 4, group A, member 2 "
3.0	TNFAIP3	"tumor necrosis factor, alpha-induced protein 3 "
3.0	VEGFA	vascular endothelial growth factor A
2.9	CEBPB	"CCAAT/enhancer binding protein (C/EBP), beta "
2.8	DEDD2	death effector domain containing 2
2.7	DNAJB6	"DnaJ (Hsp40) homolog, subfamily B, member 6 "
2.7	TNFRSF10D	"tumor necrosis factor receptor superfamily, member 10d, decoy with truncated death domain "
2.6	SOX9	SRY (sex determining region Y)-box 9
2.5	SOCS3	suppressor of cytokine signaling 3
2.4	TGM2	"transglutaminase 2 (C polypeptide, protein-glutamine-gamma-glutamyltransferase) "
2.4	TBX3	T-box 3
2.4	CLU	clusterin
2.2	FOSL1	FOS-like antigen 1
2.2	IL6R	interleukin 6 receptor
2.2	NOTCH1	notch 1
2.1	GCLM	"glutamate-cysteine ligase, modifier subunit "
2.1	CLCF1	cardiotrophin-like cytokine factor 1
2.1	SPHK1	sphingosine kinase 1
2.1	IER3	immediate early response 3
2.1	UBB	ubiquitin B
2.0	CSF2	colony stimulating factor 2 (granulocyte-macrophage)

Notes: Significant transcripts were selected when expression values changed by 2-fold.

Table 25. Classification of increased genes associated with cell survival categories

Ontology term	Count
regulation of survival gene product expression	2
B Cell Survival Pathway	2
regulation of cell proliferation	31
positive regulation of cell proliferation	20
cell proliferation	16
negative regulation of cell proliferation	12
regulation of smooth muscle cell proliferation	7
positive regulation of smooth muscle cell proliferation	5
regulation of epithelial cell proliferation	3
positive regulation of epithelial cell proliferation	2
Cadmium induces DNA synthesis and proliferation in macrophages	2
Inhibition of Cellular Proliferation by Gleevec	2

Notes: Significant transcripts were selected when expression values changed by 2-fold.

Table 26. Regulation of cell proliferation

Fold Change	Gene Symbol	Gene Description
18.1	HMOX1	heme oxygenase (decycling) 1
9.8	IL8	interleukin 8
7.8	DDR2	discoidin domain receptor tyrosine kinase 2
7.5	TRIB1	tribbles homolog 1 (Drosophila)
6.9	XIRP1	xin actin-binding repeat containing 1
6.5	NPPC	natriuretic peptide C
6.2	IL11	interleukin 11
5.4	ADAMTS1	"ADAM metallopeptidase with thrombospondin type 1 motif, 1 "
4.5	KLF10	Kruppel-like factor 10
4.5	FABP3	"fatty acid binding protein 3, muscle and heart (mammary-derived growth inhibitor) "
4.0	LIF	leukemia inhibitory factor
3.2	JUN	jun proto-oncogene
3.1	PTHLH	parathyroid hormone-like hormone
3.1	MMP12	matrix metallopeptidase 12 (macrophage elastase)
3.1	EGR4	early growth response 4
3.0	VEGFA	vascular endothelial growth factor A
2.8	ATF3	activating transcription factor 3
2.8	SERTAD1	SERTA domain containing 1
2.7	FGF18	fibroblast growth factor 18
2.6	HBEGF	heparin-binding EGF-like growth factor
2.6	SOX9	SRY (sex determining region Y)-box 9

2.4	TGM2	"transglutaminase 2 (C polypeptide, protein-glutamine-gamma-glutamyltransferase) "
2.4	TBX3	T-box 3
2.4	CLU	clusterin
2.2	FOSL1	FOS-like antigen 1
2.2	JAG1	jagged 1
2.2	IL6R	interleukin 6 receptor
2.2	NOTCH1	notch 1
2.1	CXCL1	"chemokine (C-X-C motif) ligand 1 (melanoma growth stimulating activity, alpha) "
2.1	SPHK1	sphingosine kinase 1
2.0	CSF2	colony stimulating factor 2 (granulocyte-macrophage)

Notes: Significant transcripts were selected when expression values changed by 2-fold.

Table 27. Regulation of epithelial cell proliferation

Fold Change	Gene Symbol	Gene Description
3.1	MMP12	matrix metallopeptidase 12 (macrophage elastase)
3.0	VEGFA	vascular endothelial growth factor A
2.2	NOTCH1	notch 1

Notes: Significant transcripts were selected when expression values changed by 2-fold.

Table 28. Classification of increased genes associated with inflammation categories

Ontology term	Count
inflammatory response	16
acute inflammatory response	3
Cytokines and Inflammatory Response	3
Cells and Molecules involved in local acute inflammatory response	3

Notes: Significant transcripts were selected when expression values changed by 2-fold.

Table 29. Inflammatory response

Fold Change	Gene Symbol	Gene Description
18.1	HMOX1	heme oxygenase (decycling) 1
9.8	IL8	interleukin 8
8.3	KDM6B	lysine (K)-specific demethylase 6B
4.0	FOS	FBJ murine osteosarcoma viral oncogene homolog
3.4	CYP4F11	"cytochrome P450, family 4, subfamily F, polypeptide 11 "
3.0	MMP25	matrix metallopeptidase 25
2.9	CEBPB	"CCAAT/enhancer binding protein (C/EBP), beta "
2.5	CCL26	chemokine (C-C motif) ligand 26
2.4	CLU	clusterin
2.3	HRH1	histamine receptor H1
2.2	IL6R	interleukin 6 receptor
2.1	PTAFR	platelet-activating factor receptor
2.1	CXCL1	"chemokine (C-X-C motif) ligand 1 (melanoma growth stimulating activity, alpha) "
2.1	MAP2K3	mitogen-activated protein kinase kinase 3
2.0	IRGM	"immunity-related GTPase family, M "
2.0	ITGAL	"integrin, alpha L (antigen CD11A (p180), lymphocyte function-associated antigen 1; alpha polypeptide) "

Notes: Significant transcripts were selected when expression values changed by 2-fold.

Table 30. Cytokines and Inflammatory Response

Fold Change	Gene Symbol	Gene Description
9.8	IL8	interleukin 8
6.2	IL11	interleukin 11
2.0	CSF2	colony stimulating factor 2 (granulocyte-macrophage)

Notes: Significant transcripts were selected when expression values changed by 2-fold.

Table 31. Classification of increased genes associated with apoptosis categories

Ontology term	Count
regulation of apoptosis	49
negative regulation of apoptosis	36
anti-apoptosis	29
apoptosis	25
positive regulation of apoptosis	17
induction of apoptosis	11
regulation of neuron apoptosis	5
regulation of anti-apoptosis	5
positive regulation of anti-apoptosis	4
induction of apoptosis by extracellular signals	3
positive regulation of neuron apoptosis	2
PTEN dependent cell cycle arrest and apoptosis	1
TSP-1 Induced Apoptosis in Microvascular Endothelial Cell	2
Neuropeptides VIP and PACAP inhibit the apoptosis of activated T cells	2
apoptotic mitochondrial changes	3

Notes: Significant transcripts were selected when expression values changed by 2-fold.

Table 32. Regulation of apoptosis

Fold Change	Gene Symbol	Gene Description
18.1	HMOX1	heme oxygenase (decycling) 1
10.6	NR4A1	"nuclear receptor subfamily 4, group A, member 1 "
9.7	DDIT3	DNA-damage-inducible transcript 3
4.9	SERPINB2	"serpin peptidase inhibitor, clade B (ovalbumin), member 2 "
4.5	KLF10	Kruppel-like factor 10
4.5	PMAIP1	phorbol-12-myristate-13-acetate-induced protein 1
4.4	DUSP1	dual specificity phosphatase 1
4.2	HSPA1B	heat shock 70kDa protein 1B
4.1	PIM1	pim-1 oncogene
4.0	HSPA1B	heat shock 70kDa protein 1B
4.0	HSPA1B	heat shock 70kDa protein 1B
3.9	DDIT3	DNA-damage-inducible transcript 3
3.7	UBC	ubiquitin C
3.7	BAG3	BCL2-associated athanogene 3
3.7	HSPA1B	heat shock 70kDa protein 1B
3.6	CRYAB	"crystallin, alpha B "
3.5	HSPA1B	heat shock 70kDa protein 1B // heat shock 70kDa protein 1A
3.5	HSPA1A	heat shock 70kDa protein 1A
3.4	ROCK1P1	"Rho-associated, coiled-coil containing protein kinase 1 pseudogene 1 "
3.4	HSPA9	heat shock 70kDa protein 9 (mortalin)
3.2	ANGPTL4	angiopoietin-like 4
3.2	JUN	jun proto-oncogene
3.2	HSPA1A	heat shock 70kDa protein 1A
3.2	ERN1	endoplasmic reticulum to nucleus signaling 1

3.1	HSPA1A	heat shock 70kDa protein 1A
3.1	HSPA1A	heat shock 70kDa protein 1A
3.1	HSPA1A	heat shock 70kDa protein 1A
3.1	HRK	"harakiri, BCL2 interacting protein (contains only BH3 domain) "
3.0	NR4A2	"nuclear receptor subfamily 4, group A, member 2 "
3.0	TNFAIP3	"tumor necrosis factor, alpha-induced protein 3 "
3.0	VEGFA	vascular endothelial growth factor A
2.9	CEBPB	"CCAAT/enhancer binding protein (C/EBP), beta "
2.8	DEDD2	death effector domain containing 2
2.7	DNAJB6	"DnaJ (Hsp40) homolog, subfamily B, member 6 "
2.7	TNFRSF10D	"tumor necrosis factor receptor superfamily, member 10d, decoy with truncated death domain "
2.6	SOX9	SRY (sex determining region Y)-box 9
2.5	SOCS3	suppressor of cytokine signaling 3
2.4	TGM2	"transglutaminase 2 (C polypeptide, protein-glutamine-gamma-glutamyltransferase) "
2.4	TBX3	T-box 3
2.4	CLU	clusterin
2.2	FOSL1	FOS-like antigen 1
2.2	IL6R	interleukin 6 receptor
2.2	NOTCH1	notch 1
2.1	GCLM	"glutamate-cysteine ligase, modifier subunit "
2.1	CLCF1	cardiotrophin-like cytokine factor 1
2.1	SPHK1	sphingosine kinase 1
2.1	IER3	immediate early response 3
2.1	UBB	ubiquitin B
2.0	CSF2	colony stimulating factor 2 (granulocyte-macrophage)

Notes: Significant transcripts were selected when expression values changed by 2-fold.

Table 33. Apoptotic mitochondrial changes

Fold Change	Gene Symbol	Gene Description
4.5	PMAIP1	phorbol-12-myristate-13-acetate-induced protein 1
3.2	JUN	jun proto-oncogene
2.4	CLU	clusterin

Notes: Significant transcripts were selected when expression values changed by 2-fold.

Table 34. Classification of increased genes associated with ROS categories

Ontology term	Count
response to reactive oxygen species	8
response to oxidative stress	11
Oxidative Stress Induced Gene Expression Via Nrf2	3
cellular response to oxidative stress	2
ion binding	74
magnesium ion binding	10
metal ion binding	74
transition metal ion binding	58
zinc ion binding	49
calcium ion binding	14
iron ion binding	7
copper ion binding	6
cadmium ion binding	6
manganese ion binding	3

Notes: Significant transcripts were selected when expression values changed by 2-fold.

Table 35. Response to oxidative stress

Fold Change	Gene Symbol	Gene Description
18.1	HMOX1	heme oxygenase (decycling) 1
9.7	DDIT3	DNA-damage-inducible transcript 3
4.4	DUSP1	dual specificity phosphatase 1
4.0	FOS	FBJ murine osteosarcoma viral oncogene homolog
3.9	DDIT3	DNA-damage-inducible transcript 3
3.6	CRYAB	"crystallin, alpha B "
3.2	JUN	jun proto-oncogene
3.0	SRXN1	sulfiredoxin 1
2.4	CLU	clusterin
2.2	FOSL1	FOS-like antigen 1
2.1	GCLM	"glutamate-cysteine ligase, modifier subunit "

Notes: Significant transcripts were selected when expression values changed by 2-fold.

Table 36. Ion binding

Fold Change	Gene Symbol	Gene Description
25.7	DNAJA4	"DnaJ (Hsp40) homolog, subfamily A, member 4 "
22.7	MMP10	matrix metallopeptidase 10 (stromelysin 2)
18.5	DLL1	delta-like 1 (Drosophila)
18.1	HMOX1	heme oxygenase (decycling) 1
16.2	SNAI1	snail family zinc finger 1
12.8	MT1B	metallothionein 1B
12.7	MT1E	metallothionein 1E
10.6	NR4A1	"nuclear receptor subfamily 4, group A, member 1 "
10.3	MMP3	"matrix metallopeptidase 3 (stromelysin 1, progelatinase) "
9.7	SLC30A1	"solute carrier family 30 (zinc transporter), member 1 "
8.9	GEM	GTP binding protein overexpressed in skeletal muscle
8.7	ZFAND2A	"zinc finger, AN1-type domain 2A "
8.3	KDM6B	lysine (K)-specific demethylase 6B
6.8	MT1G	metallothionein 1G
5.4	ADAMTS1	"ADAM metallopeptidase with thrombospondin type 1 motif, 1 "
5.1	CHORDC1	cysteine and histidine-rich domain (CHORD) containing 1
5.1	MT1M	metallothionein 1M
5.1	ASTL	astacin-like metallo-endopeptidase (M12 family)
4.7	SIK1	salt-inducible kinase 1
4.7	CDH16	"cadherin 16, KSP-cadherin "
4.5	KLF10	Kruppel-like factor 10
4.1	PIM1	pim-1 oncogene
4.1	IDI2	isopentenyl-diphosphate delta isomerase 2
3.9	GCM1	glial cells missing homolog 1 (Drosophila)

3.8	NR4A3	"nuclear receptor subfamily 4, group A, member 3 "
3.7	UBC	ubiquitin C
3.6	RYBP	RING1 and YY1 binding protein
3.5	ZBTB2	zinc finger and BTB domain containing 2
3.4	CYP4F11	"cytochrome P450, family 4, subfamily F, polypeptide 11 "
3.4	ROCK1P1	"Rho-associated, coiled-coil containing protein kinase 1 pseudogene 1 "
3.3	JHDM1D	jumonji C domain containing histone demethylase 1 homolog D (S. cerevisiae)
3.2	EGR3	early growth response 3
3.2	ERN1	endoplasmic reticulum to nucleus signaling 1
3.2	ZC3H12A	zinc finger CCCH-type containing 12A
3.1	PTHLH	parathyroid hormone-like hormone
3.1	MMP1	matrix metallopeptidase 1 (interstitial collagenase)
3.1	MMP12	matrix metallopeptidase 12 (macrophage elastase)
3.1	MT1F	metallothionein 1F
3.1	EGR4	early growth response 4
3.0	NR4A2	"nuclear receptor subfamily 4, group A, member 2 "
3.0	TNFAIP3	"tumor necrosis factor, alpha-induced protein 3 "
3.0	TES	testis derived transcript (3 LIM domains)
3.0	MMP25	matrix metallopeptidase 25
3.0	SRXN1	sulfiredoxin 1
2.9	ZNF34	zinc finger protein 34
2.9	ZSWIM6	"zinc finger, SWIM-type containing 6 "
2.9	ABL2	v-abl Abelson murine leukemia viral oncogene homolog 2
2.8	TET3	tet methylcytosine dioxygenase 3
2.7	EDEM2	"ER degradation enhancer, mannosidase alpha-like 2 "
2.7	NQO2	"NAD(P)H dehydrogenase, quinone 2 "

2.5	SCUBE2	"signal peptide, CUB domain, EGF-like 2 "
2.4	RLF	rearranged L-myc fusion
2.4	TGM2	"transglutaminase 2 (C polypeptide, protein-glutamine-gamma-glutamyltransferase) "
2.3	ALOXE3	arachidonate lipoxygenase 3
2.3	ACSL5	acyl-CoA synthetase long-chain family member 5
2.3	MT1X	metallothionein 1X
2.3	B3GNT2	"UDP-GlcNAc:betaGal beta-1,3-N-acetylglucosaminyltransferase 2 "
2.2	RARA	"retinoic acid receptor, alpha "
2.2	JAG1	jagged 1
2.2	ZNF274	zinc finger protein 274
2.2	NOTCH1	notch 1
2.2	ZCCHC6	"zinc finger, CCHC domain containing 6 "
2.2	CARS	cysteinyl-tRNA synthetase
2.2	PHF13	PHD finger protein 13
2.2	TIPARP	TCDD-inducible poly(ADP-ribose) polymerase
2.1	HIC1	hypermethylated in cancer 1
2.1	JMJD1C	jumonji domain containing 1C
2.1	ZNF469	zinc finger protein 469
2.1	SPHK1	sphingosine kinase 1
2.1	UBB	ubiquitin B
2.0	KLF6	Kruppel-like factor 6
2.0	CYP2B7P1	"cytochrome P450, family 2, subfamily B, polypeptide 7 pseudogene 1 "
2.0	HIVEP1	human immunodeficiency virus type I enhancer binding protein 1
2.0	ITGAL	"integrin, alpha L (antigen CD11A (p180), lymphocyte function-associated antigen 1; alpha polypeptide) "

Notes: Significant transcripts were selected when expression values changed by 2-fold.

3.3.4. Effects of silver NPs on cytokine production and inflammatory response

Cytokine production in BEAS-2B cells treated with 5 nm and 100 nm silver NPs was assessed by ELISA. Epithelial cells were treated with different concentrations of silver NPs for 8 h (Figure 13A) and 24 h (Figure 13B). Because IL-8 is an earlier-responding cytokine, the two experiments used different treatment times. Supernatants harvested from control and cells treated with silver NPs were assayed for IL-8 and IL-11. IL-8 production was highest in the 0.5 μg/mL treatment, at 1,413 pg/mL; at higher concentrations of silver NPs, cell death was induced. IL-11 production was highest in the 0.75 μg/mL treatment, at 3,733 pg/mL. As predicted, treatment with 100 nm silver NPs did not increase IL-8 and IL-11 release. These results suggest that expression of cytokines in response to silver NPs is size- and dose-dependent in epithelial cells. Furthermore, these results support the results of the cDNA microarray analysis.
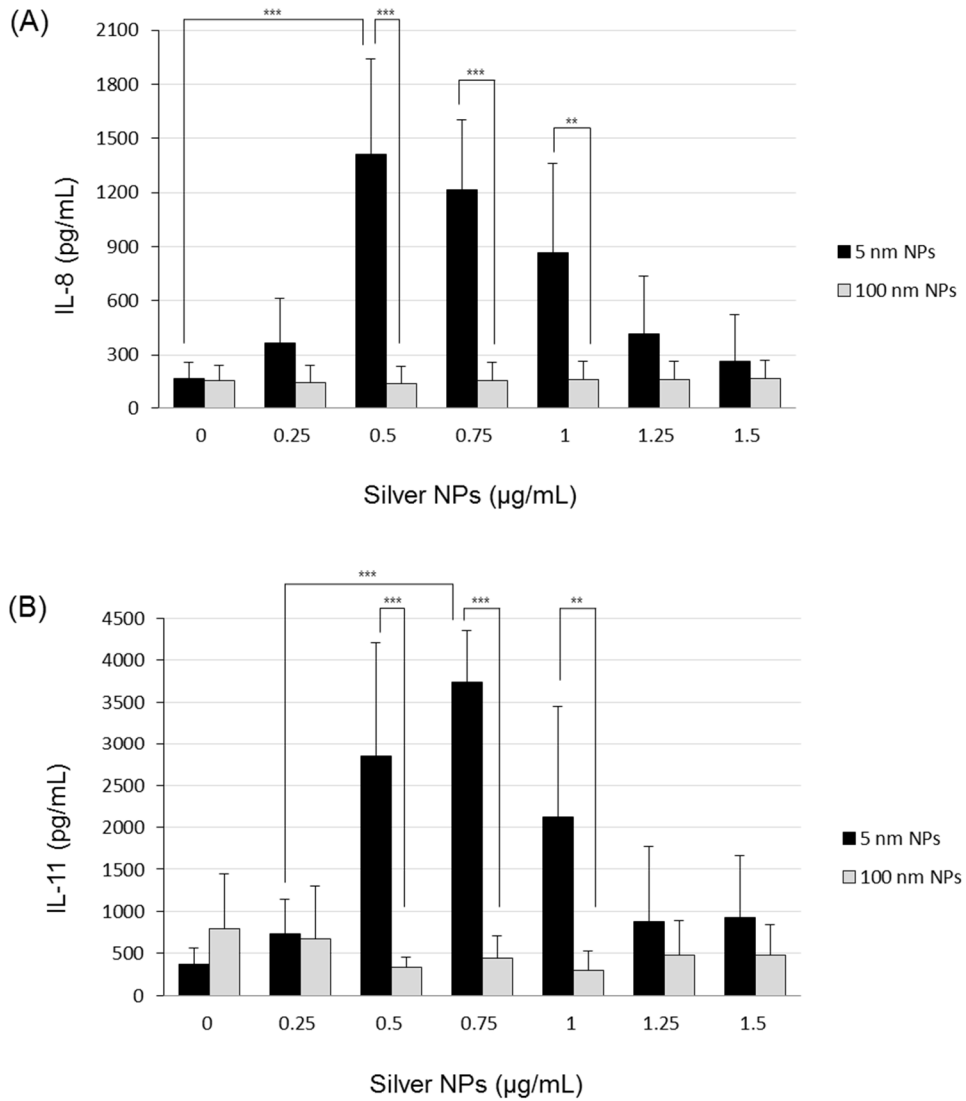
Figure 13. Dose-dependent expression of cytokines in response to silver NPs. (A) BEAS-2B cells treated with different doses of silver NPs for 8 h. (B) BEAS-2B cells treated with different doses of silver NPs for 24 h. Culture supernatant was harvested and levels of IL-8 and IL-11 were measured by ELISA. Treatment with 5 nm silver NPs induced IL-8 release,

but treatment with 100 nm silver NPs did not. Data represent the mean ±
SD of three independent experiments. One-way and two-way ANOVA
analyses were used to determine significance (**p < 0.01, ***p < 0.001).

3.3.5. Expression of genes related to cytokine production and ROS

Real-time RT-PCR analysis was performed for IL-8, which was found to be significantly increased in the cDNA microarray analysis, and for IL-11, HSP70, and HO-1. Real-time RT-PCR analysis was performed for 6 h with 0.25 to 0.75 μg/mL of silver NPs. At concentrations ranging from 0.25 to 0.75 μg/mL, IL-8 gene expression increased by 2.8-, 20.6-, and 21.6-fold, respectively. At the same concentrations, IL-11 gene expression increased by 1.3-, 11.5-, and 15.6-fold, respectively (Figure 14A). In addition, at the same doses, HSP70 gene expression increased by 16-, 85.6-, and 103.2-fold, respectively. Lastly, at these concentrations, HO-1 gene expression increased by 54.9-, 243.5-, and 163-fold, respectively (Figure 14B). In concordance with the microarray data, expression of genes related to cytokine production and ROS increased after treatment with 5 nm silver NPs. However, 100 nm silver NPs did not increase the expression of IL-8, IL-11, HSP70, or HO-1. These results indicate that the results of the microarray and real-time RT-PCR analyses are concordant.
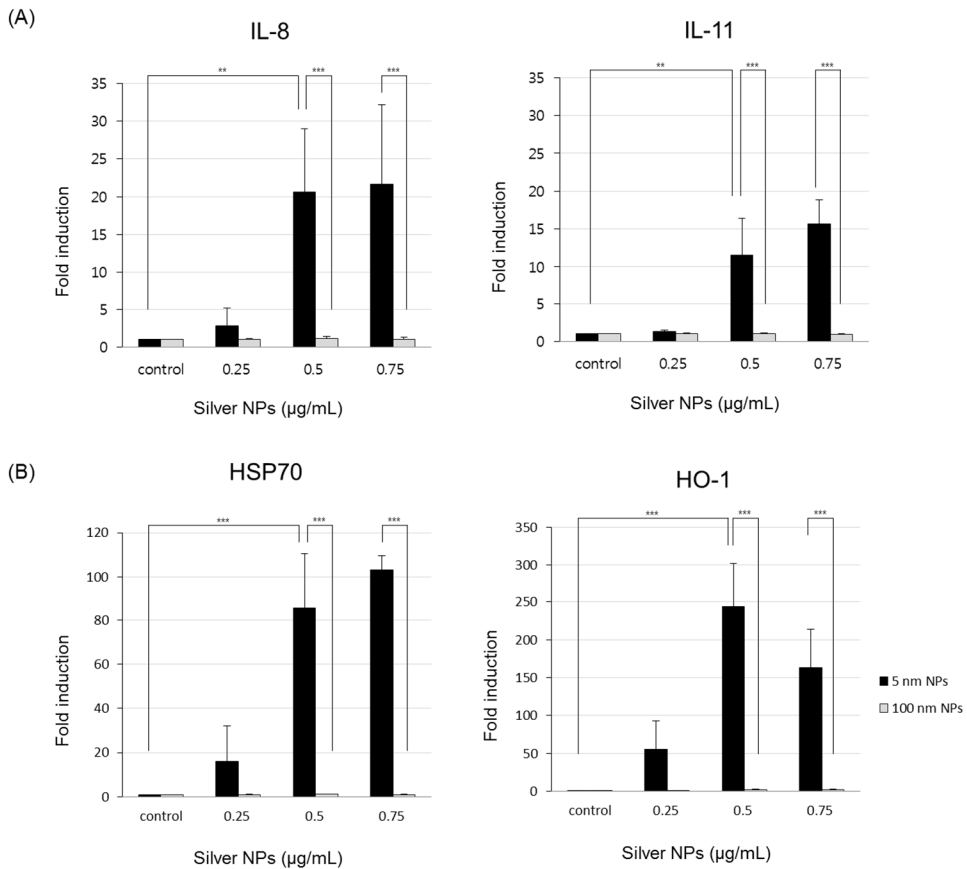
(A)

(B)

Figure 14. Expression of genes related to cytokine production and ROS in bronchial epithelial cells treated with silver NPs. (A) Real−time RT−PCR analysis was performed for 6 h at 0.25 μg/mL to 0.75 μg/mL of silver NPs. Expression of genes related to cytokine production increased after treatment with 5 nm silver NPs, but not after treatment with 100 nm silver NPs. (B) Expression of ROS−related genes. Real−time RT−PCR analysis was performed for 6 h at 0.25 μg/mL to 0.75 μg/mL of silver NPs. Exposure to 5 nm silver NPs induced increased expression of HSP70 and HO−1. Exposure to 100 nm silver NPs did not induce increased expression

of HSP70 and HO-1. Real-time RT-PCR was performed three times and representative data are shown. Data are shown as the mean ± SD of three or more independent experiments. One-way and two-way ANOVA analyses were used to determine significance (**p < 0.01, ***p < 0.001).

3.3.6. Effects of silver NPs on HSP70 and HO-1 expression

Two proteins (HSP70 and HO-1) were chosen for further analysis using western blotting, based on increased expression in response to treatment with 5 nm silver NPs. In accordance with the realtime-PCR results showed that RNA levels of HSP70 increased to a maximum of 103.2-fold and HO-1 increased to a maximum of 243.5-fold at 6 h-exposure. Therefore we tested the effect of silver NPs on the expression of HSP70 and HO-1 protein in BEAS-2B cells. BEAS-2B cells were treated with different doses of silver NPs for 24 h. Each 30-μg protein sample was loaded and analyzed with anti-HSP70, anti-HO-1, and anti-GAPDH (loading control) antibodies. HSP70 and HO-1 expression increased in cells treated with high-dose silver NPs compared to untreated cells. HSP70 protein levels increased by a maximum of 7.7-fold at 0.5 μg/mL and HO-1 protein levels increased by a maximum of 8.9-fold at the same concentration, compared to untreated cells (Figure 15). In contrast, ROS-associated proteins were not affected by treatment with 100 nm silver NPs. These results suggest that exposure to silver NPs could increase the expression of proteins related to oxidative stress.
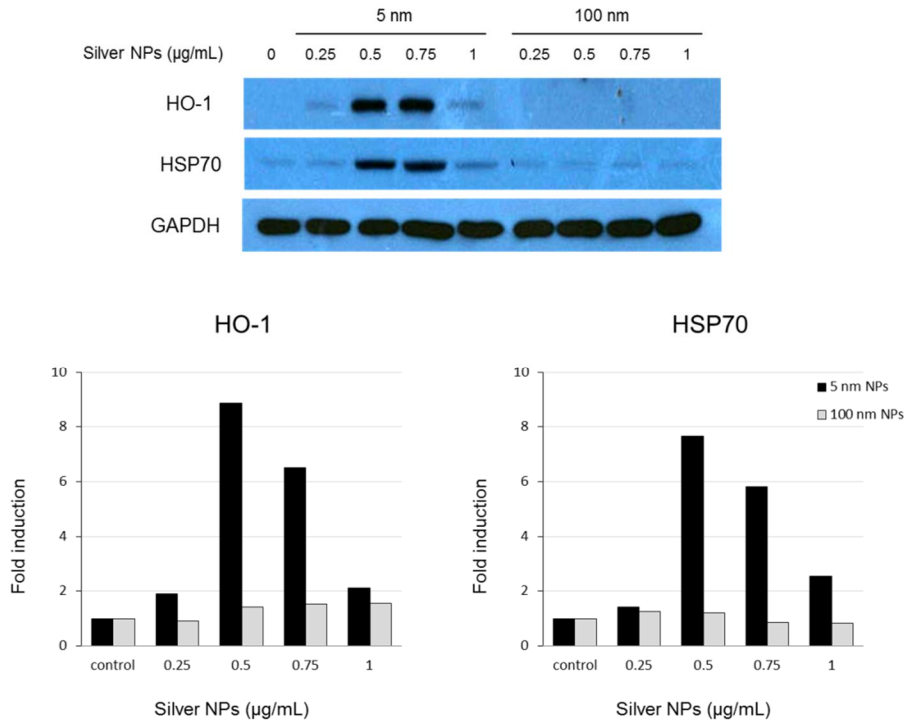
Figure 15. Protein levels of HSP70 and HO−1 in bronchial epithelial cells treated with silver NPs. BEAS−2B cells were treated with different doses of silver NPs for 24 h. Each 30−μg protein sample was analyzed using anti−HSP70, anti−HO−1, and anti−GAPDH (loading control) antibodies.

4. Discussion

Today, engineered nanomaterials are being applied and used in various consumer products. In particular, the use of silver NPs has gradually increased due to its antimicrobial and unique physical characteristics. However, a growing number of studies report that silver NPs are toxic to the human due to the small size of its particles. Since the potential health impact of nanomaterials increases with the rapid growth of nano-industry, it is important to fully investigate the safety of and their potential hazards (2).

In this study, the safety of silver NPs was investigated by examining the effect of silver NPs on endothelial and epithelial cells. Most previous studies anticipated that NP inhalation mainly affects the epithelial cells of respiratory tissues. However, studies verify that NPs introduced through the respiratory system are found in various other organs outside of the respiratory system (21). This means that it can penetrate through epithelial cells to endothelial cells due to its extremely small size. Endothelial cells are cells surrounding blood vessels, and nanoparticles penetrating into endothelial cells can affect various organs through blood stream.

First, we evaluated the cytotoxic effects of silver NPs in endothelial and epithelial cells. Although the LD_{50} of each cell line was estimated differently, the toxicity of silver NPs was proven. However, for 100 nm

silver NPs, cell death was not observed in the high concentration group (endothelial cells: 3.5 ㎍/mL; epithelial cells: 1.5 ㎍/mL). It can therefore be suggested that the cytotoxicity of silver NPs depends on the size of particles and on the treatment dose. In a prior study, we evaluated the effect of silver NPs in macrophage cells. It was verified through microarray that 5 nm silver NPs affect the variation of gene expression in cells, and a noticeable increase in the expression of the IL-8 gene and of oxidative-stress related gene in early time was also verified (11). Similarly, we were also able to verify that the expression of not only oxidative stress-related genes but also inflammatory response-related genes increased in response to exposure to 5 nm silver NPs in both endothelial and epithelial cells. Oxidative stress-induced ROS is produced in cell death or early time before cellular damage (49). We also found variation in oxidative stress-related genes in early after exposure, among which the variation in metallothionein (MT), heme oxygenase 1 (HO-1), and heat shock 70kDa protein (HSP70) were especially noticeable. In one earlier study, 20-50 nm silver NPs were added to A549 cells, producing oxidative stress products such as malondialdehyde (MDA) and 8-hydroxy-2'-deoxyguanosine (8-oxo-dG) and consequently increasing levels of HSP and HO-1 (50). This is similar to the results of our study. Our study has proven that HSP70, HO-1, and MT are sufficient as biomarkers of ROS and that the oxidative stress effect increases as NP size decreases, given that there is no variation in ROS related gene expression following exposure to 100 nm

1 1 1

silver NPs.

  The microarray used in this study can analyze up to 24,838 RefSeq (Entrez) genes. Based on the results of this analysis, genes undergoing intracellular change after exposure to silver NPs were classified into five categories: cell death, cell survival, inflammation, apoptosis, and ROS. As a result, there was considerable variation in genes related to cell death and apoptosis, and the expression of genes related to cell survival was also significant. Meanwhile, the number of genes related to inflammation was relatively small. This is supported by our review of previous research, which showed that only IL-8 gene expression among cytokines increased shortly after the exposure of macrophage cells to 5 nm silver NPs (11). However, this study was increased with the addition to the IL-8, IL-11, IL-1α and IL-36α into endothelial cells. In epithelial cells, the only intracellular cytokines that increased following exposure to 5 nm of silver NPs were IL-8 and IL-11. In addition, ROS-related genes were the most marked as ion binding ontology terms. It might be because silver NPs are gradually ionized to Ag$^+$ over time, and accordingly the variation of ion-binding related genes developed actively. A previous study has suggests that toxicity is generated by free silver ions induced by silver NPs, but this is a combined effect of silver ions and silver NPs (51).

  One point especially worth paying attention to is the increased IL-11 gene expression, which has not been greatly discussed in previous studies. In this study, the expression of the IL-11 gene particularly increased

following exposure to 5 nm silver NPs in both endothelial cells and epithelial cells. IL-11 increases the frequency and proportion of proliferating megakaryocytes in bone marrow. This role of IL-11 in bone marrow failure syndromes, such as aplastic anemia and myelodysplastic syndrome, is being investigated in clinical trials. IL-11 also stimulates myeloid and erythroid differentiation and regulates macrophage precursors. Its potential in treating mild hemophilia A is suggested. As an anti-inflammatory cytokine, IL-11 has been identified as having immunomodulatory activities by reducing pro-inflammatory cytokine synthesis. Based on the pivotal role of IL-11 in inflammatory conditions, it has been investigated as a candidate for treating rheumatoid arthritis, Crohn's disease, refractory immune thrombocytopenic purpura, and periodontal disease (52). Thus IL-11 has various functions, and it roles can vary by cell type (48). One study suggests that IL-11 is involved in cell proliferation in endothelial cells. The study indicates that IL-11 is related to the STAT3 pathway, and accordingly surviving proteins are expressed and have a positive effect on cell proliferation (53). However, considering that this study's microarray results showed increased expression of 31 genes including IL-11 in epithelial cells as well as 20 genes including IL-11 in endothelial cells, which were classified as ontology term as regulation of cell proliferation, it was inferred that IL-11 plays a role in cell proliferation not only in endothelial cells but also in epithelial cells. Moreover, IL-11 is classified as an anti-inflammatory

cytokine, and the microarray results for endothelial cells showed a 10.4－ fold increase in its expression, which was much higher than other cytokines. This also might have affected the proliferation of endothelial cells. In addition, genes whose ontology terms classify them as regulating apoptosis showed an increased expression of 37 in endothelial cells and 49 in epithelial cells. Although IL－11 is associated with apoptosis and thus induces cell death in both endothelial and epithelial cells, it stimulates more genes in epithelial cells. This is supported by earlier studies, that argued that one of the various functions of IL－11 is induction of apoptosis in epithelial cells (54, 55, 56). Given the great variety of roles played by IL－ 11, it is difficult to determine its role in a specific cell. Therefore, although this study has verified that IL－11 expression commonly increases in cells due to the influence of silver NPs, additional studies using various methods will be required in the future, as the specific roles played by IL－11 can vary by cell type.

5. Conclusions

A summary of this study's results is as follows:

1. Endothelial and epithelial cell viability was dependent on silver NP particle size. Cell death was induced by 5 nm silver NPs. The viability of cells treated with 5 nm and 100 nm silver NPs differed.

2. The number of genes whose expression increased due to silver NPs was much higher in the 5 nm treatment group than in the 100 nm group. This also proves that smaller NPs have stronger toxicity.

3. The genes that increased greatly following exposure to silver NPs were mainly oxidative stress effect-related genes such as MT, HO-1, and HSP70, and this is related to the induction of cellular toxicity by silver NPs following the ROS pathway.

4. The cytokines increased by exposure to silver NPs were IL-8 and IL-11. The expression of these cytokines increased even early following exposure, which does not have high cellular toxicity. It can be assumed that early after exposure the inflammatory response action and the anti-inflammatory response act at the same time.

5. IL-11 has exhibits many different functions, and, its roles appear to vary by cell types. IL-11 can induce apoptosis by exacerbating inflammation and can also regulate cell proliferation.

6. Silver NPs create a toxic effect response in both endothelial and epithelial cells. They also stimulate genes involved in cell activities such as cell death, cell survival, inflammation, apoptosis, and oxidative stress.

7. After treatment with 5 nm silver NPs, mitochondrial swelling, a decrease or disappearance of cytoplasm, and vacuolization were observed. But after treatment with 100 nm silver NPs, no clear changes in cell morphology were observed except for the presence of NPs in lysosomes and the nucleus.

In conclusion, this study finds that intracellular genes specifically respond to exposure to silver NPs, and among cytokines the expression of IL-11 is especially significant. It also finds that toxic effect is affected by the size of NPs. However, this study only verifies that IL-11 expression increased; further study will be required to in order to elucidate the various roles played by IL-11.

6. References

1. Whitesides GM, Mathias JP, Seto CT. Molecular self-assembly and nanochemistry: a chemical strategy for the synthesis of nanostructures. Science. 1991;254(5036):1312-9.

2. Mohammad CHAREH SAZ. Toxicologic evaluation of silver nanoparticles. Hacettepe university institute of health science. 2014.

3. Huang BC, Notten AD, Rasters N. Nanoscience and Technology Publications and Patents: A Review of Social Science Studies and Search Strategies. The Journal of Technology Transfer. 2011;36(2):145-172.

4. Ju-Nam Y, Lead JR. Manufactured Nanoparticles: An Overview of Their Chemistry, Interactions and Potential Environmental Implications. Science of the Total Environment. 2008;400:396-414.

5. Tran QH, Nguyen VQ. Le AT. Silver Nanoparticles: Synthesis, Properties, Toxicology, Applications and Perspectives. Advances in Natural Sciences: Nanoscience and Nanotechnology. 2013;4:1-20.

6. Stevenson APZ, Bea DB, Civit S, Contera SA, Cerveto AI, Trigueros S. Three Strategies to Stabilise Nearly Monodispersed Silver Nanoparticles in Aqueous Solution. Nanoscale Research Letters. 2012;7(151):1-8.

7. Vance ME, Kuiken T, Vejerano EP, McGinnis SP, Hochella MF Jr, Rejeski D, Hull MS. Nanotechnology in the real world: Redeveloping

the nanomaterial consumer products inventory. Beilstein J Nanotechnol. 2015;6:1769-80.

8. Asharani PV, Hande MP, Valiyaveettil S. Anti-proliferative activity of silver nanoparticles. BMC Cell Biol. 2009;10:65.

9. Su CL, Chen TT, Chang CC, Chuang KJ, Wu CK, Liu WT, Ho KF, Lee KY, Ho SC, Tseng HE, Chuang HC, Cheng TJ. Comparative proteomics of inhaled silver nanoparticles in healthy and allergen provoked mice. Int J Nanomedicine. 2013;8:2783-99.

10. El-Badawy AM, Silva RG, Morris B, Scheckel KG, Suidan MT, Tolaymat TM. Surface charge-dependent toxicity of silver nanoparticles. Environ Sci Technol. 2011;45(1):283-7.

11. DaeHyoun L, Jiyoung J, Seungjae K, Taegyeong K, Kangtaek L, In-Hong C. The effects of sub-lethal concentrations of silver nanoparticles on inflammatory and stress genes in human macrophages using cDNA microarray analysis. Biomaterials. 2012;33:4690-4699.

12. Mi Jin L, Seung Jun L, Su Jin Y, Ji-Young J, Hangoo K, Kyongmin K, In-Hong C, Sun P. Silver nanoparticles affect glucose metabolism in hepatoma cells through production of reactive oxygen species. Int J Nanomedicine. 2015;22:11:55-68.

13. Hussain SM, Hess KL, Gearhart JM, Geiss KT, Schlager JJ. *In Vitro* Toxicity of Nanoparticles in BRL 3 A Rat Liver Cells. Toxicology *in Vitro*. 2005;19:975-983.

14. Piao MJ, Kang KA, Lee IK, Kim HS, Kim S, Choi JY, Choi J, Hyun JW. Silver Nanoparticles Induce Oxidative Cell Damage in Human Liver Cells through Inhibition of Reduced Glutathione and Induction of Mitochondria-Involved. Toxicology Letters. 2011;201:92-100.

15. Ucciferri N, Collnot EM, Gaiser BK, Tirella A, Stone V, Domenici C, Lehr CM, Ahluwalia A. *In Vitro* Toxicological Screening of Nanoparticles on Primary Human Endothelial Cells and The Role of Flow in Modulating Cell Responce. Nanotoxicology. 2014;8(6):697-708.

16. Martínez-Gutierrez F, Thi EP, Silverman JM, de Oliveira CC, Svensson SL, Vanden Hoek A, Sánchez EM, Reiner NE, Gaynor EC, Pryzdial EL, Conway EM, Orrantia E, Ruiz F, Av-Gay Y, Bach H. Antibacterial activity, inflammatory response, coagulation and cytotoxicity effects of silver nanoparticles. Nanomedicine: Nanotechnology, Biology, and Medicine. 2012;8: 328-336.

17. Park J, Lim DH, Lim HJ, Kwon T, Choi JS, Jeong S, Choi IH, Cheon J. Size dependent macrophage responses and toxicological effects of Ag nanoparticles. Chemical Communications. 2011;47:4382-4384.

18. Greulich C, Diendorf J, Gessmann J, Simon T, Habijan T, Eggeler G, Schildhauer TA, Epple M, Köller M. Cell Type-Specific Responses of Peripheral Blood Mononuclear Cells to Silver Nanoparticles. Acta Biomaterialia. 2011;7:3505-3514.

19. Fischer HC, Chan WC. Nanotoxicity: the growing need for *in vivo* study. Current Opinion in Biotechnology. 2007;18:565-571.

20. Johnston HJ, Hutchison G, Christensen FM, Peters S, Hankin S, Stone V. A review of the *in vivo* and *in vitro* toxicity of silver and gold particulates: particle attributes and biological mechanisms responsible for the observed toxicity. 2010;40(4):328-346.

21. Park EJ, Bae E, Yi J, Kim Y, Choi K, Lee SH, Yoon J, Lee BC, Park K. Repeated-dose toxicity and inflammatory responses in mice by oral administration of silver nanoparticles. Environ Toxicol Pharmacol. 2010;30(2):162-8.

22. Vander Zande M, Vandebriel RJ, Van Doren E, Kramer E, Herrera Rivera Z, Serrano-Rojero CS, Gremmer ER, Mast J, Peters RJ, Hollman PC, Hendriksen PJ, Marvin HJ, Peijnenburg AA, Bouwmeester H. Distribution, elimination, and toxicity of silver nanoparticles and silver ions in rats after 28-day oral exposure. Oral Exposure. ACS Nano. 2012;6(8):7427-7442.

23. Muth-Köhne E, Sonnack L, Schlich K, Hischen F, Baumgartner W, Hund-Rinke K, Schäfers C, Fenske M. The toxicity of silver nanoparticles to zebrafish embryos increases through sewage treatment processes. Ecotoxicology. 2013;22(8):1264-77.

24. Shimada A, Kawamura N, Okajima M, Kaewamatawong T, Inoue H, Morita T. Translocation pathway of the intratracheally instilled

ultrafine particles from the lung into the blood circulation in the mouse. Toxicol Pathol. 2006;34(7):949-57.

25. Wu JT1, Wu LL. Linking inflammation and atherogenesis: Soluble markers identified for the detection of risk factors and for early risk assessment. Clin Chim Acta. 2006;366(1-2):74-80.

26. Bartłomiejczyk T, Lankoff A, Kruszewski M, Szumiel I. Silver nanoparticles – allies or adversaries? Ann Agric Environ Med. 2013;20(1):48-54.

27. Hightower LE. Heat shock, stress proteins, chaperones, and proteotoxicity. Cell. 1991;66(2):191-197.

28. Yao X, Bai Q, Yan D, Li G, Lü C, Xu H. Solanesol protects human hepatic L02 cells from ethanol-induced oxidative injury via upregulation of HO-1 and Hsp70. Toxicol *In Vitro*. 2015;29(3):600-8.

29. Truettner JS, Hu K, Liu CL, Dietrich WD, Hu B. Subcellular stress response and induction of molecular chaperones and folding proteins after transient global ischemia in rats. Brain Res. 2009;1249:9-18.

30. Singh MP, Reddy MM, Mathur N, Saxena DK, Chowdhuri DK. Induction of hsp70, hsp60, hsp83 and hsp26 and oxidative stress markers in benzene, toluene and xylene exposed Drosophila melanogaster: role of ROS generation. Toxicol Appl Pharmacol. 2009;235(2):226-43.

31. Xin L, Li X, Deng H, Kuang D, Dai X, Huang S, Wang F, He M, Currie RW, Wu T. Development of stable HSPA1A promoter-driven

luciferase reporter HepG2 cells for assessing the toxicity of organic pollutants present in air. Cell Stress Chaperones. 2012;17(5):567-76.

32. Paine A, Eiz-Vesper B, Blasczyk R, Immenschuh S. Signaling to heme oxygenase-1 and its anti-inflammatory therapeutic potential. Biochem Pharmacol. 2010;80(12):1895-903.

33. Lee DS, Li B, Kim KS, Jeong GS, Kim EC, Kim YC. Butein protects human dental pulp cells from hydrogen peroxide-induced oxidative toxicity via Nrf2 pathway-dependent heme oxygenase-1 expressions. Toxicol *In Vitro*. 2013;27(2):874-81.

34. Lee TS, Chau LY. Heme oxygenase-1 mediates the anti-inflammatory effect of interleukin-10 in mice. Nat Med. 2002;8(3):240-6.

35. Neubauer JA, Sunderram J. Heme oxygenase-1 and chronic hypoxia. Respir Physiol Neurobiol. 2012;184(2):178-85.

36. Ryter SW, Alam J, Choi AM. Heme oxygenase-1/carbon monoxide: from basic science to therapeutic applications. Physiol Rev. 2006;86(2):583-650.

37. Zhang JM, An J. Cytokines, inflammation, and pain. Int Anesthesiol Clin. 2007;45(2):27-37.

38. Taga T, Kishimoto T. Gp130 and the interleukin-6 family of cytokines. Annu Rev Immunol. 1997;15:797-819.

39. Putoczki TL, Thiem S, Loving A, Busuttil RA, Wilson NJ, Ziegler PK, Nguyen PM, Preaudet A, et al. Interleukin-11 is the dominant IL-6

family cytokine during gastrointestinal tumorigenesis and can be targeted therapeutically. Cancer Cell. 2013;24(2):257-71.

40. Schwertschlag US, Trepicchio WL, Dykstra KH, Keith JC, Turner KJ, Dorner AJ. Hematopoietic, immunomodulatory and epithelial effects of interleukin-11. Leukemia. 1999;13(9):1307-15.

41. Wan B, Zhang H, Fu H, Chen Y, Yang L, Yin J, Wan Y, Shi Y. Recombinant human interleukin-11 (IL-11) is a protective factor in severe sepsis with thrombocytopenia: A case-control study. Cytokine. 2015;76(2):138-43.

42. Putoczki T, Ernst M. More than a sidekick: the IL-6 family cytokine IL-11 links inflammation to cancer. J Leukoc Biol. 2010;88(6):1109-17.

43. Du X, Everett ET, Wang G, Lee WH, Yang Z, Williams DA. Murine interleukin-11 (IL-11) is expressed at high levels in the hippocampus and expression is developmentally regulated in the testis, J. Cell. Physiol. 1996;168(2);362-372.

44. Du X, Williams DA. Interleukin-11: review of molecular, cell biology, and clinical use. Blood. 1997;89(11):3897-908.

45. Musashi M, Yang YC, Paul SR, Clark SC, Sudo T, Ogawa M. Direct and synergistic effects of interleukin 11 on murine hemopoiesis in culture. Proc Natl Acad Sci U S A. 1991;88(3):765-9.

46. Hill GR, Cooke KR, Teshima T, Crawford JM, Keith JC Jr, Brinson YS,

Bungard D, Ferrara JL. Interleukin-11 promotes T cell polarization and prevents acute graft-versus-host disease after allogeneic bone marrow transplantation. J Clin Invest. 1998;102(1):115-23.

47. Howlett M, Chalinor HV, Buzzelli JN, Nguyen N, van Driel IR, Bell KM, Fox JG, Dimitriadis E, Menheniott TR, Giraud AS, Judd LM. IL-11 is a parietal cell cytokine that induces atrophic gastritis. Gut. 2012;61(10):1398-409.

48. Xu DH, Zhu Z, Wakefield MR, Xiao H, Bai Q, Fang Y. The role of IL-11 in immunity and cancer. Cancer Lett. 2016;373(2):156-163.

49. Dröge W. Oxidative stress and aging. Adv Exp Med Biol. 2003;543:191-200.

50. Xin L, Wang J, Wu Y, Guo S, Tong J. Increased oxidative stress and activated heat shock proteins in human cell lines by silver nanoparticles. Hum Exp Toxicol. 2015;34(3):315-23.

51. Beer C, Foldbjerg R, Hayashi Y, Sutherland DS, Autrup H. Toxicity of silver nanoparticles - nanoparticle or silver ion? Toxicol Lett. 2012;208(3):286-92.

52. Negahdaripour M, Nezafat N, Ghasemi Y. A panoramic review and in silico analysis of IL-11 structure and function. Cytokine Growth Factor Rev. 2016.

53. Mahboubi K, Li F, Plescia J, Kirkiles-Smith NC, Mesri M, Du Y, Carroll JM, Elias JA, Altieri DC, Pober JS. Interleukin-11 up-regulates

survivin expression in endothelial cells through a signal transducer and activator of transcription-3 pathway. Lab Invest. 2001;81(3):327-34.

54. Putoczki T, Ernst M. More than a sidekick: the IL-6 family cytokine IL-11 links inflammation to cancer. J Leukoc Biol. 2010;88(6):1109-17.

55. Ernst M, Putoczki TL. Molecular pathways: IL11 as a tumor-promoting cytokine-translational implications for cancers. Clin Cancer Res. 2014;20(22):5579-88.

56. Johnstone CN, Chand A, Putoczki TL, Ernst M. Emerging roles for IL-11 signaling in cancer development and progression: Focus on breast cancer. Cytokine Growth Factor Rev. 2015;26(5):489-98.

ABSTRACT (in KOREAN)

사람 내피세포와 기관지 상피세포에서

은 나노입자에 의한 인터루킨 11 과 스트레스 유전자의 증가

장 지 영

연세대학교 대학원 나노메디컬협동과정

(지도교수 최 인 홍)

초미립자 나노물질의 크기는 약 100 nm 정도로 이러한 작은 크기의 특성으로 인하여 산업적으로 여러 방면에서 활용이 되고 있다. 그 중 은 나노입자는 항균작용의 영향으로 의학분야에서 많이 활용되고 있다. 그러나 최근들어 은 나노입자가 인체에 유해한 영향을 미치는 원인물질로 지목되면서 많은 연구자들이 은 나노입자 뿐만 아니라 전반적인 나노입자에 대한 독성 평가와 위해성 평가를 진행하고 있다.

본 연구에서는 은 나노입자를 사람 내피세포와 상피세포로 구분하여 일정시간 노출시킨 후 관찰되는 여러가지 세포 반응들을 확인하고자 하였다. 은

나노입자에 의해 세포내 산화적 스트레스가 발생하여 세포사멸이 진행되고 어떠한 유전자들이 자극을 받아 변화가 관찰되는지 확인해 보고자 하였다. 그리고 나노입자에 노출 된 후 세포 내 여러 유전자들의 발현 양상의 변화를 마이크로어레이 기법을 통하여 확인하였다.

연구 결과, 사람 내피세포와 상피세포 에서 반치사농도 값은 각각 다르게 산출되었지만 공통적으로 5 nm 은 나노입자에 대한 세포독성이 확인되었다. 나노입자처럼 크기가 작은 물질은 세포내부로 침투하여 사멸을 유도하는데 5 nm 은 나노입자는 세포 내부로 침투하여 세포질을 파괴하는 것을 확인하였지만 100 nm 은 나노입자는 세포내부로 일부의 입자가 침투되기는 하나 세포 손상을 일으키지는 않았다. 은 나노입자의 노출로 인하여 세포 내에서 발현이 증가하는 유전자의 개수는 100 nm 보다 5 nm 에서 월등히 많이 확인되었다. 은 나노입자에 의하여 증가 발현의 폭이 큰 유전자들은 대표적으로 메탈로티오닌 (MT, metallothionein), 헴 옥시게나아제 1 (HO-1, heme oxygenasae 1), 열 충격 단백질 70 (HSP70, heat shock 70kDa protein)과 같이 주로 산화적 스트레스와 관련된 유전자이며 이는 은 나노입자가 주로 활성산소 기전을 따라 세포독성이 유도되는 것과 연관된다. 그리고 은 나노입자에 의해 증가되는 주된 사이토카인은 인터루킨 8 과 11 이었으며 세포독성이 크지 않은 노출초기에도 이들 사이토카인의 발현이 증가되었다. 이는 노출 초기에도 염증반응이 작용하며 동시에 항염증반응 또한 작용함을 추측할 수 있었다. 이와 같이 은 나노입자는 사람 내피세포와 상피세포 모두에서 독성 반응을 유발하였으며 세포사멸, 세포증식, 염증반응, 산화적 스트레스 등 세포활성에 관여하는 전반적인 유전자들을 자극시켰다.

결론적으로, 본 연구에서는 은 나노입자가 세포에 노출되면 세포내 유전자들이 특이적으로 반응을 한다는 것과 사이토카인들 중에서 특별히 인터루킨 11 의 발현이 두드러짐을 발견하였다. 그리고 세포에 대한 독성 영향은 나노입자의 크기와 깊은 연관이 있음을 재확인하였다. 하지만 이번 연구에서는 은 나노입자에 의하여 인터루킨 11 이 증가 발현이 되었다는 현상만 확인되었을 뿐이므로 향후 추가적으로 인터루킨 11 의 다양한 역할을 입증할 수 있도록 여러 방면에서 추가연구가 진행되어야 할 것이다.

핵심어: 은, 나노입자, 내피세포, 상피세포, 인터루킨-11

Publication List

1. **Jang J**, Lim DH, Choi IH. The impact of nanomaterials in immune system. Immune Netw. 2010;10(3):85-91.

2. Kim S, **Jang J**, Kim H, Choi H, Lee K, Choi IH. The effects of silica nanoparticles in macrophage cells. Immune Netw. 2012;12(6):296-300.

3. Lim DH, **Jang J**, Kim S, Kang T, Lee K, Choi IH. The effects of sub-lethal concentrations of silver nanoparticles on inflammatory and stress genes in human macrophages using cDNA microarray analysis. Biomaterials. 2012;33(18):4690-4699.
   (Co-first author)

4. Yang EJ, **Jang J**, Kim S, Choi IH. Silver Nanoparticles as a Smart Antimicrobial Agent. Journal of Bacteriology and Virology. 2012;42(2):177 – 179.

5. Yang EJ, **Jang J**, Lim DH, Choi IH. Enzyme-linked immunosorbent assay of IL-8 production in response to silver nanoparticles. Methods Mol Biol. 2012;926:131-9.

6. Yang JY, Kim JY, **Jang JY**, Lee GW, Kim SH, Shin DC, Lim YW. Exposure and Toxicity Assessment of Ultrafine Particles from Nearby Traffic in Urban Air in Seoul, Korea. Environ Health Toxicol. 2013;28:e2013007.

7. Ann SJ, Chung JH, Park BH, Kim SH, **Jang J**, Park S, Kang SM, Lee SH.

PPARα agonists inhibit inflammatory activation of macrophages through upregulation of β-defensin 1. Atherosclerosis. 2015;240(2):389-97.

8. Lee MJ, Lee SJ, Yun SJ, **Jang J**, Kang HG, Kim K, Choi IH, Park S. Silver nanoparticles affect glucose metabolism in hepatoma cells through production of reactive oxygen species. Int J Nanomedicine. 2016;11:55-68.

9. Kang HG, **Jang J**, Choi IH. Immunotoxicity of Metal Oxide and Metal Nanoparticles and Animal Models to Evaluate Immunotoxicity of Nanoparticles. Current Bionanotechnology, 2016;2(2): 84-90.